KINETIC STUDIES OF OROTATE PHOSPHORIBOSYLTRANSFERASE FROM BAKER'S YEAST

by

JACOB VICTOR

A dissertation submitted to the Graduate Faculty in Biochemistry in partial fulfillment of the requirements for the degree of Doctor of Philosophy, The City University of New York.

1978

This manuscript has been read and accepted for the Graduate Faculty in Biochemistry in satisfaction of the dissertation requirement for the degree of Doctor of Philosophy.

7/28/18
date

Chairman of Examining Committee

8/3/18
date

Executive Officer

Supervisory Committee

The City University of New York

Abstract

Kinetic Studies of Orotate Phosphoribosyltransferase

from Baker's Yeast

by

Jacob Victor

Adviser: Professor Donald L. Sloan

Kinetic analysis of the reaction catalyzed by a homogeneous preparation of orotate phosphoribosyltransferase from yeast has revealed that the reaction proceeds by a bibi ping-pong kinetic mechanism. This conclusion is based on initial rate measurements and product inhibition studies of both the forward phosphoribosyl transfer and the reverse pyrophosphorylation reactions in the presence of an optimal concentration of magnesium ion. Each half reaction was characterized using labeled $^{14}[C]$-orotate and $^{32}[P]$-PP_i and the enzyme was shown to catalyze an exchange of label, between $^{14}[C]$-orotate and OMP in the absence of PRPP, and between $^{32}[P]$-PP_i and PRPP in the absence of orotate. Divalent magnesium ion was shown to be essential for both isotope exchange reactions. The physiological phosphoribosyl transfer reaction is initiated by the formation of an activated phosphoribosyl-enzyme intermediate from phosphoribosyl 1'-pyrophosphate (PRPP) with the release of pyrophosphate (PP_i) from the α 1'-position. The second half of the reaction involves the formation of a β 1'-glycosidic bond between orotate and the ribose phosphate moiety on the enzyme to form orotidine 5'-phosphate (OMP).

Michaelis constants (K_m) for PRPP, orotate, PP_i and OMP were determined to be 38 ± 8 μM, 22 ± 6 μM, 96 ± 6 μM and 8 ± 2 μM, respectively. V_{max} for the forward direction was 28.5 μM OMP/min /mg of protein, and 31.3 μM OMP/min /mg of protein for the reverse direction. The utilization of 5-fluoro-orotate produced parallel initial velocity plots and a K_m value of PRPP analogous to those observed with orotate. A K_m value of 24 ± 5 μM calculated for fluoro-orotate was similar to the value determined for orotate. Product inhibition constants (K_i) for all of the reactants were calculated from the kinetic data for both the forward and reverse reactions. Attempts to isolate the proposed phosphoribosyl-enzyme intermediate were inconclusive. EPR and PRR studies using Mn^{2+} detected metal binary complexes with PRPP, PP_i, OMP and enzyme.

Because stereochemical inversion results from the overall reaction, this ping-pong reaction must involve a mechanism more complicated than a double displacement. Possible mechanisms consistent with the kinetic and exchange data are discussed.

ACKNOWLEDGEMENTS

This thesis is dedicated to my father, my son, Aaron, and most of all, my dear wife, Irene, whose love, devotion, and encouragement have helped bring this work to its successful completion.

I would like to thank the members of my thesis committee, Dr. Sharon Cosloy, Dr. Thomas Haines, Dr. Horst Schultz, and Dr. William Sweeney for their time, cooperation and valuable advice.

I would also like to thank Larry Greenberg for performing one of the pyrophosphate product inhibition studies; and Bruce Trig and Alice Hershey for their aid in isolating the OPRTase enzyme.

A special acknowledgement must be extended to Dr. Sweeney for allosing us access to the ESR facility at Hunter College.

Finally, I would like to thank my mentor, Dr. Donald Sloan, for all the guidance, patience, and encouragement he has shown me during every phase of this work.

Wondrous are Thy works;
And that, my soul knoweth exceedingly.

Psalms 139:14

TABLE OF CONTENTS

LIST OF TABLES

LIST OF FIGURES

INTRODUCTION

In all organisms that have been studied (1) the de novo synthesis of uridine-5'-phosphate (UMP) from orotate involves two enzymes. First, orotate phosphoribosyltransferase (OPRTase, EC 2.4.2.10), catalyzing the stereospecific formation of a β-glycosidic bond between orotate and the ribose-5'-phosphate moiety of 5'-phosphoribosyl α1'-pyrophosphate (PRPP), forms orotidine 5'-phosphate (OMP) and pyrophosphate (PP_i) as products (Figure 1, equation 1). OMP is then decarboxylated by orotidine-5'-phosphate decarboxylase (ODCase, EC 4.1.1.23) to give UMP (Figure 1, equation 2).

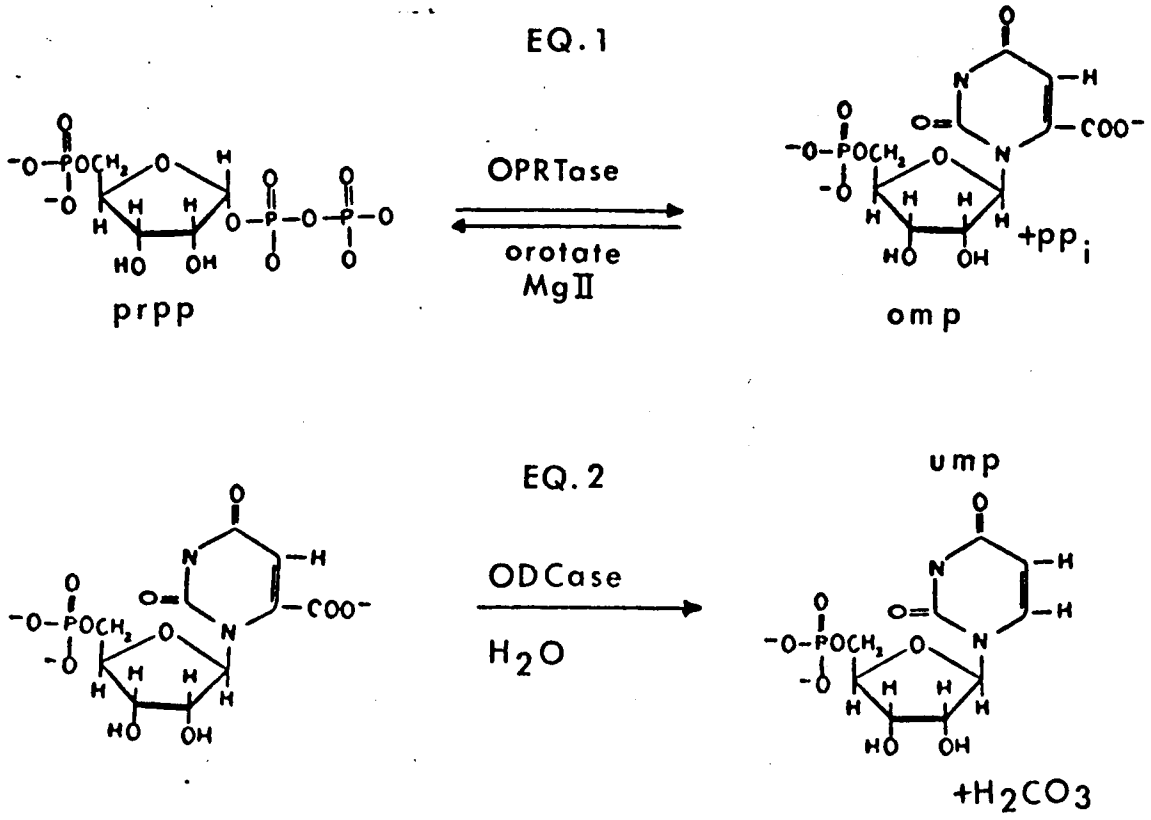

Figure 1. Reactions catalyzed by OPRTase and ODCase.

OPRTase displays an absolute requirement for magnesium or manganese ion (2), although copper has been able to replace magnesium in wheat embryos (3). ODCase, however, does not require metals for its activity (4).

These two enzymes have been shown to copurify from all mammalian tissues studied to date. These include bovine brain (5), erythrocytes (6, 7) and calf thymus (8), Ehrlich ascites carcinoma (9), and murine leukemia P1534J (10). The two enzymes also show a coordinate relationship (that is, an effect on one enzyme activity will be closely paralleled on the other) in rat (11, 12), adult and developing mouse liver and heart (13), human diploid cell strains (14) and erythrocytes, and various other mammalian erythrocytes (15). In view of these findings it is now generally believed that OPRTase and ODCase exist as a bifunctional enzyme complex.

In the absence of ODCase activity the phosphoribosyl transfer reaction has been shown to be reversible. This has been demonstrated in yeast (4) as well as in rat liver and Morris hepatomas (11). One of the consequences of OPRTase and ODCase existing in a complex would be to render irreversible the formation of UMP from orotate. This pyrophosphorylase activity should not be significant in-vivo because of the presence of inorganic pyrophosphatases which leave little if any pyrophosphate available for the reaction (16).

The advantage of such a multienzyme complex might be to channel the first substrate (orotate) directly to the final product (UMP) without significantly accumulating the intermediate (OMP). This effect has been demonstrated in mouse Ehrlich ascites cells (17), mouse liver and murine leukemia P1534J (18). This was not the case

with the yeast enzymes where OMP was observed to accumulate while UMP was being synthesized (18). The OPRTase-ODCase complex is thought not to exist in yeast because the two enzymes have been separated and isolated to homogeneous states (4). There is some controversy as to the makeup of the mammalian complex. The complex from murine leukemia P1534J could be separated only by mild proteolysis with papain (10), and the enzymes from Ehrlich ascites cells always cosediment suggesting a single multifunctional protein (17, 21, 22). However, the OPRTase and ODCase activity of the calf thymus complex were separated using starch gel electrophoresis (8). Human erythrocyte complex is dissociable and is composed of an ODCase dimer and an OPRTase dimer (19). Mouse liver cell free extracts, containing the OPRTase-ODCase complex, after being stored at -20°C for two weeks, were no longer eluted together from DEAE-biogel A and were separated by chromatography on G-150 (21). Upon separation the enzymes lose activity or become more labile, particularly the OPRTase. This is in contrast to the yeast enzymes where ODCase is the more labile of the two (4). The complex isolated from Serratia marcescens has been shown to contain dihydroorotase (DHOase) as well as OPRTase and ODCase activities. This complex can be dissociated completely to give the three enzymic activities. While there are large losses in activity, when OPRTase and ODCase are recombined both activities are restored fully (21). The complex appears to either stabilize the individual enzyme activities or is essential for maximal activity; but whether one multifunctional protein or two enzymes is the rule in mammalian systems is still unclear.

OPRTase is a potential site of control for pyrimidine nucleotide biosynthesis. It was shown to be the rate limiting step in Ehrlich

ascites cells (22), rat hepatoma cells (23) and rat liver (24). The gene (pyrE) which codes for OPRTase has been located for Escherchia coli (25) and found to be unlinked to the other genes of the pyrimidine pathway, including ODCase. This is true also for Baker's yeast (26), Neurospora crassa (27) and Salmonella typhimurium (28) as demonstrated by OPRTase levels that do not change in response to the level of the pyrimidine pool or to the pool of precursor metabolites. On the other hand, ODCase activity levels respond to both precursors (orotic acid, carbamyl aspartic acid and dihydroorotic acid) and the pyrimidine pool. Regulation of enzyme biosynthesis in E. coli is via repression-derepression by a pyrimidine metabolite (29, 30), while the mammalian complex and ODCase of yeast are regulated by induction (26, 31). (OPRTase activity is relatively constant and seems to show little gene regulation 21, 26.)

How these two enzymes are regulated in humans has been studied by examining mutants. Deficiencies of OPRTase and ODCase activities are characteristics of hereditary orotic aciduria, a potentially lethal inborn error of pyrimidine metabolism in man. Two variant forms of the disease have been described; one having a deficiency of both OPRTase and ODCase (Type I) and the other lacking ODCase while exhibiting elevated OPRTase levels (Type II) (31). The disease manifests itself as severe anemia, retardation and excessive orotic acid in the urine (32).

Observation of the effects of pyrimidine analogs demonstrated induction as the mode of regulation for the mammalian enzymes. Azauridine, azaorotic or barbituric acids, placed in the medium surrounding fibroblasts from patients with either type of orotic aciduria raised

the low enzyme or both enzyme activities ten to fifty-fold (32). The same effect, somewhat reduced, is seen in fibroblasts from normal individuals. This increase was shown not to be due to a dissociable activator or inhibitor in the extracts, and the increase occurs even when sufficient cytidine is present in the medium to permit optimal growth. The effect, therefore, cannot be due to repression-derepression but can be accounted for by induction.

Nucleotides or pyrimidine analogs which can bind to the complex appear to increase the in-vivo stability of the two enzymes. The drug allopurinol induces elevated levels of OPRTase and ODCase. Levels of the two enzymes decrease normally in a coordinate fashion, but twice as slowly in the presence of allopurinol. Allopurinol must be conferring greater stability to the complex.

The coordinate behavior of the two enzymes led to the suggestion that the genes coding for them could be linked and, as a result, hereditary orotic aciduria could arise from a defect in the regulator gene of the two enzymes (32). As we have mentioned, the two enzyme activities may reside on a single polypeptide protein. Both types of orotic aciduria can then be explained more simply by a single structural gene coding for a single protein with both activities. Type I orotic aciduria would arise from a totally inactive gene product, whereas type II would lack a correct base in that portion of the gene crucial for the active site of ODCase and will not affect the OPRTase activity (21). A complex involving two proteins can also account for both diseased states (19). Since the complex is essential for activity, a structural defect of the decarboxylase subunit, preventing the formation of an active complex, will leave both enzymes

unbound and inactive. For type II orotic aciduria, the ability to form the complex remains, but a defect in the catalytic activity of ODCase occurs. To date, the genetic data does not clarify whether the complex is a single protein or two separable enzymes.

PRPP is the common metabolite for all phosphoribosyltransferases (PRTase). The true substrate for all the enzymes is thought to be the monomagnesium complex of PRPP (17). The dimagnesium salt of PRPP was believed to be the substrate for human hypoxanthine PRTase (33), but later it was shown that the monomagnesium complex is the actual substrate, and the dimagnesium salt was, in fact, inhibitory (34).

The intracellular concentration of PRPP has a critical role in the regulation of purine metabolism in man. Increased PRPP levels are found in patients with gout and Lesch-Nyhan syndrome (these involve a hypoxanthine-guanine PRTase deficiency). Hereditary orotic aciduria does not display an elevated PRPP level, and it is believed, therefore, that OPRTase only utilizes a small portion of the available PRPP (35). The PRPP levels in human erythrocytes range from 1 to 5 uM. These values are substantially lower than the Km's of most PRTases (35). Thus the concentration of PRPP within the cell may be an important factor in the regulation of de-novo purine and pyrimidine biosynthesis. In fact, cellular PRPP regulates its own eventual utilization by activating carbamyl phosphate synthetase, the first enzyme in the de-novo synthesis of UMP. A more direct relationship between OPRTase and PRPP levels has been demonstrated by the effects of allopurinol and orotic acid. Allopurinol, a drug that causes the depletion of intracellular PRPP, increases the in-vivo levels of OPRTase (14, 36). Orotic acid, the other substrate of OPRTase, decreases the level of PRPP in-vivo, and inhibits de-novo purine metabolism, as well (35).

In view of OPRTase's involvement with ODCase, purine biosynthesis, intracellular PRPP levels and hereditary orotic aciduria, it would be desirable to obtain a clearer understanding of how OPRTase operates. Its kinetic mechanism is totally unknown (37). Any mechanistic study in the mammalian system requires the addition of an inhibitor of ODCase to even detect the pyrophosphorylase activity. Therefore, OPRTase from yeast, which is readily separable from ODCase activity, is ideal for detailed kinetic studies of both the phosphoribosyl transfer and pyrophosphorylation reactions. In this paper we present the purification, kinetic analysis, and substrate binding studies of OPRTase from Bakers' yeast. The results are consistent with a bibi ping-pong kinetic mechanism.

THEORY

Ping-Pong Kinetics

A mechanism by which a product is released between the addition of two substrates has been termed ping-pong (38). If we illustrate the OPRTase reaction in terms of the Cleland notation, the reversible reaction can be illustrated as follows:

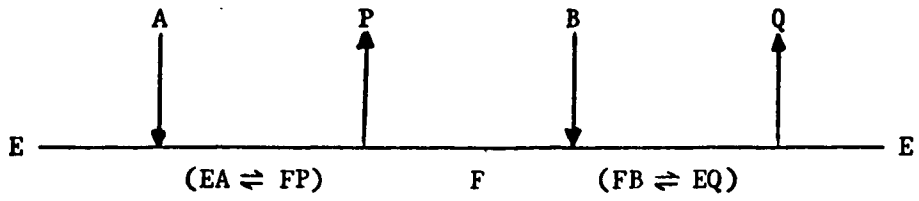

where E = free enzyme

EA = enzyme-substrate (PRPP) complex

FP = the ribose phosphate enzyme product (PP_i) complex

F = the ribose-phosphate enzyme

FB = the ribose-phosphate enzyme substrate (orotate) complex

EQ = the enzyme product (OMP) complex

In the absence of products the initial velocity patterns will yield a series of parallel lines consistent with equations 3 and 4.

$$\frac{1}{v} = \frac{K_{m_A}}{V_{max}} \frac{1}{[A]} + \frac{1}{V_{max}} \left(1 + \frac{K_{m_B}}{[B]}\right) \qquad (3)$$

$$\frac{1}{v} = \frac{K_{m_B}}{V_{max}} \frac{1}{[B]} + \frac{1}{V_{max}} \left(1 + \frac{K_{m_A}}{[A]}\right) \qquad (4)$$

These families of parallel lines do not necessarily indicate a ping-pong mechanism because under some conditions, lines that seem parallel are not due to a ping-pong system. In an ordered bibi system in which the K_{ia} is very much smaller than the K_{mA} (when the K_{ia} to K_{mA} ratio is less than 0.1, a deviation from parallel lines cannot be detected graphically (39)), the reciprocal velocity plots will intersect far to the left of the 1/v axis and far below the 1/A axis, but these lines will appear to be parallel in the region of interest. Moreover, this effect will be observed whether substrate [A] or substrate [B] is varied. An example of this phenomenon was observed with phosphofructokinase from Dictostelium discoidem (40). The similarity between the ping-pong and ordered mechanisms can be seen quite readily from the initial velocity equations. When K_{ia} is very much smaller than K_{mA} the equation for an ordered system (equation 5) reduces to the same expression as that for the ping-pong mechanism (equation 4).

$$\frac{1}{v} = \frac{K_{mB}}{V_{max}}\left(1 + \frac{K_{ia}}{[A]}\right)\frac{1}{[B]} + \frac{1}{V_{max}}\left(1 + \frac{K_{mA}}{[A]}\right) \qquad (5)$$

Parallel patterns also emerge from a rapid random equilibrium mechanism when the binding of one substrate inhibits the binding of the other. This has been observed with the enzyme Protein kinase from Neurospora crassa (41). In non-rapid equilibrium random systems, such as Rabbit Muscle Phosphofructokinase (42), the rate constants for the release of A and B are lower than V_{max} in the forward direction. Although the reciprocal plots are really concave upward, they appear parallel in the graphical region which characterizes K_{mA} and K_{mB}.

Product inhibition patterns can distinguish between these "masked" ordered and random mechanisms and a true ping-pong mechanism. Table I lists the predicted product inhibition patterns for each of the kinetic mechanisms we have mentioned.

To confirm that the parallel patterns are due to a ping-pong mechanism, the following product inhibition studies must be carried out. When [A] (PRPP) is varied in the presence of various levels of fixed, unsaturating concentrations of B (orotate), and in the presence of P (PP_i), a non-competitive pattern of lines should emerge from both ordered and ping-pong mechanisms. The observation of a non-competitive pattern rules out a rapid equilibrium random mechanism for this enzymic reaction. When [A] is varied in the presence of various fixed, unsaturated concentrations of B, and in the presence of Q (OMP), a competitive pattern should emerge for a ping-pong and an ordered mechanism. This observation eliminates the possibility of a non-rapid equilibrium random mechanism. To differentiate between ordered and ping-pong mechanisms, [B] must be varied in the presence of fixed, unsaturating concentrations of A, and in the presence of P. A competitive pattern will be observed if the mechanism is ping-pong, whereas a mixed-type pattern will indicate an ordered mechanism. The product inhibition patterns for a ping-pong system emerge from the following equations; for varied [A] in the presence of P (equation 6) and Q (equation 7), and when [B] is varied at fixed A with P (equation 8) and Q (equation 9).

$$\frac{v}{V_{max}} = \frac{[A]}{K_{m_A}\left(1+\frac{K_{ia}K_{m_B}[P]}{K_{m_A}K_{ip}[B]}\right)+[A]\left(1+\frac{K_{m_B}[P]}{K_{ip}[B]}+\frac{K_{m_B}}{[B]}\right)} \qquad (6)$$

Table I. Product Inhibition Patterns (adapted from Segel, 43)

Mechanism	Product Inhibitor	Varied A Unsaturated with B	Varied B Unsaturated with A
Ordered Bibi	P	MT	MT
	Q	C	MT
Rapid Equilibrium Random Bibi	P	C	C
	Q	C	C
Non-rapid Equilibrium Random Bibi	P	MT	MT
	Q	MT	MT
Ping-Pong Bibi	P	MT	C
	Q	C	MT

(C = competitive pattern, MT = mixed type or non-competitive pattern)

$$\frac{v}{V_{max}} = \frac{[A]}{K_{m_A}\left(1 + \frac{K_{ib}[Q]}{K_{iq}[B]} + \frac{[Q]}{K_{iq}}\right) + [A]\left(1 + \frac{K_{m_B}}{[B]}\right)} \qquad (7)$$

$$\frac{v}{V_{max}} = \frac{[B]}{K_{m_B}\left(1 + \frac{K_{ia}[P]}{K_{ip}[A]} + \frac{[P]}{K_{ip}}\right) + [B]\left(1 + \frac{K_{m_A}}{[A]}\right)} \qquad (8)$$

$$\frac{v}{V_{max}} = \frac{[B]}{K_{m_B}\left(1 + \frac{K_{ib}K_{m_A}[Q]}{K_{m_B}K_{iq}[A]}\right) + [B]\left(1 + \frac{K_{m_A}}{[A]} + \frac{K_{m_A}[Q]}{K_{iq}[A]}\right)} \qquad (9)$$

Perhaps the strongest diagnostic test for a ping-pong mechanism is demonstrating isotopic exchange between A and P, or between B and Q in the absence of the other substrates. A possible ping-pong mechanism for OPRTase can be illustrated by the half-reactions shown in equations 10 and 11.

$$E + PRPP \rightleftharpoons E\text{-}RP + PP_i \qquad (10)$$

$$E\text{-}RP + Orotate \rightleftharpoons E + OMP \qquad (11)$$

Thus, a demonstration that labeled PP_i will exchange with PRPP in the presence of catalytic amounts of enzyme, but in the absence of orotate and OMP, indicates a ping-pong system. However, if no exchange is detected, the mechanism is probably a masked ordered or random mechanism.

The exchange velocity equation (equation 12, for varied $[A^*]$ at different, fixed levels of $[P]$) (44) for an isolated portion of a

ping-pong mechanism yields a parallel pattern of reciprocal plots similar to the initial velocity patterns.

$$\frac{v^*}{V^*_{max_{A-P}}} = \frac{[A^*][P]}{K_m[P] + K_{ip}[A] + [A][P]} \qquad (12)$$

From the above discussion, it is clear that more than one criteria must be utilized to establish a enzymatic kinetic mechanism. In order to conclude that a reaction proceeds through the use of a ping-pong mechanism, the following observations must be made: 1) the initial velocity patterns must be composed of parallel straight lines for both substrates (and for all substrates of a reversible reaction), 2) the product inhibition patterns must fit those described in Table I, and 3) each half-reaction (as illustrated by equations 10 and 11) must be observed to proceed through the use of radioactive-label exchange techniques.

Electron Spin Resonance (EPR)

The ability of EPR to detect and characterize the presence of unpaired electrons has been employed previously to study the interactions of divalent paramagnetic manganous ion (Mn^{2+}), with various substrates and enzymes (45).

An explanation of the theory describing this important analytical technique is as follows. When an electromagnetic wave of energy, $h\nu$, irradiates a paramagnetic ion in a direction perpendicular to a static magnetic field, a magnetic dipolar transition takes place between the split states and resonance absorption of the electromagnetic energy will occur. The energy absorbed in a transition of this nature is recorded as a function of the magnetic field giving the resultant EPR spectrum.

The energy gap between the two electron spin states is expressed by equation 13 (where H is the applied magnetic field, β is the Bohr magneton, and g is the spectroscopic splitting factor, with an approximate value of 2).

$$E = g \beta H = h\nu$$

There are two further types of splitting. Zero field splitting arises where the atom or molecule concerned possesses more than one unpaired electron. In the case of Mn^{2+}, where $M_s = 5/2$, we find splitting into six M_s levels corresponding to $\pm 5/2$, $\pm 3/2$, and $\pm 1/2$. The number of allowable transitions for these six levels are five (the selection rule requires $M_s = \pm$Integer). Hyperfine splitting is due to the interaction of the unpaired electron and the magnetic moment of the nucleus. Mn^{2+} has a magnetic moment with a nuclear spin of $I = 5/2$. The number of hyperfine lines produced reflect the $(2I + 1)$ different orientations of the nuclear spin, yielding six hyperfine lines for the Mn^{2+} ESR spectra. The five zero field splitting groups will all be split into six lines each by hyperfine splitting but only one group will be detected as the four other sets will average each other out due to angular variations (46, 47).

For our purposes EPR will be used to detect binary complexes of the OPRTase system. The aqueous Mn^{2+} spectrum consists of a signal with 6 hyperfine components that show a g-value of about 2, and can be assigned to the cation Mn^{2+} surrounded by 6 molecules of water. The observed Mn^{2+} EPR spectrum in H_2O at room temperature is illustrated in Figure 2 (46). It has been shown that the complexation of Mn^{2+} to various ligands decreases the amplitude of Mn^{2+} EPR signal proportional to the free metal concentration (48). It was concluded

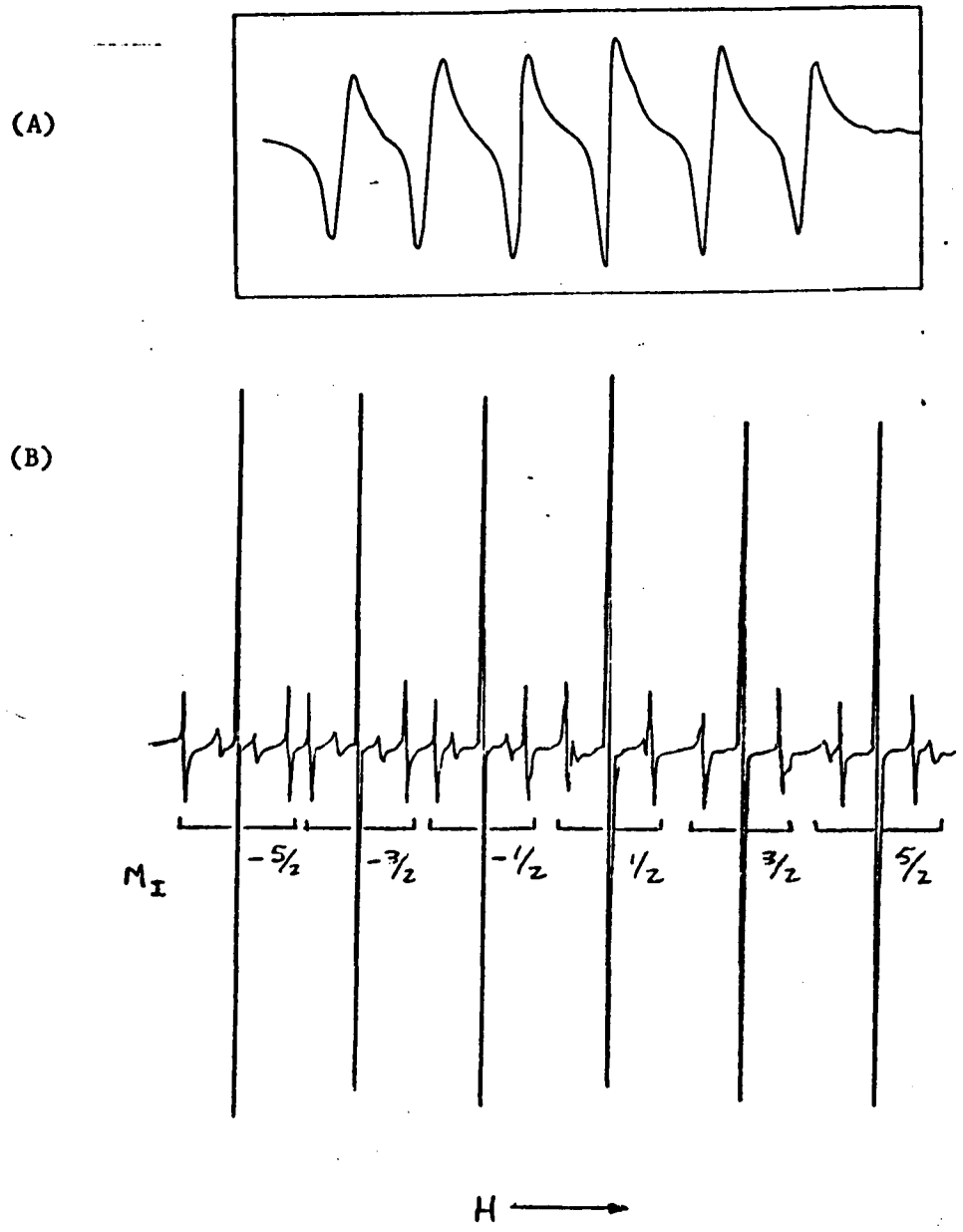

Figure 2A. The observed Mn^{2+} EPR spectrum in H_2O at room temperature. B. Mn^{2+} powder EPR spectrum in MgO at room temperature, showing six sets of quintets due to hyperfine and zero field splitting. (From Electron Spin Resonance by Wertz, J. E. and Bolton, J. R. (1972), p. 308, McGraw-Hill, New York,)

from this previous work that titrations of OPRTase and the various substrates with Mn^{2+} would yield a binding isotherm, if complexation takes place, as evidenced by a decrease in signal amplitude. To be sure, Mn^{2+} has been shown to replace Mg^{2+} as the divalent metal activator of the reaction catalyzed by OPRTase (4), and therefore, the use of Mn^{2+} to study the role of metal in OPRTase catalyzed reactions by ESR techniques will be studies of a kinetically viable system.

Proton Resonance Relaxation (PRR)

The effect of Mn^{2+} on the longitudinal nuclear relaxation rate of water protons ($1/T_1$) can be used to determine the extent of ligand binding to the metal. The values of this parameter are expressed in terms of enhancement (e_b), which is the ratio of the proton relaxation of Mn^{2+} $(ligand)_n(H_2O)_{6-n}$ to that of Mn^{2+} $(H_2O)_6$ at the same metal ion concentration (49).

Any atomic nucleus with an odd number of protons or neutrons has a net magnetic moment, and its magnetic vector will tend to orient in a magnetic field. The longitudinal relaxation time (T_1) is the first-order time constant for establishing this orientation, and its reciprocal (T_1^{-1}) is the first-order longitudinal relaxation rate (50).

Magnetic nuclei undergo relaxation by interacting with and exchanging magnetic energy with their environment. For transfers of magnetic energy to occur (which leads to spin lattice or longitudinal relaxation), the magnetic environment or "lattice" must be capable of absorbing energy which fluctuates at the Larmor (precession) frequency of the magnetic nucleus at a given field. The fluctuation of magnetic interaction between protons is caused by molecular tumbling (10^{11} sec^{-1}), and because there are large differences between tumbling frequency and the

Larmor frequency, the transfer of magnetic energy occurs at a slow rate (T_1 = 2.4 sec. for water) (49).

The perturbation of a nuclear spin system caused by the presence of unpaired electrons changes the magnitude of the nuclear longitudinal relaxation time, T_1. The paramagnetic contribution to T_1, T_{1p}, is shown in equation 14, where p is the ratio of the concentration of the paramagnetic species (Mn^{2+}) to that of the water molecules (H^1 of water), q is the number of the coordinated magnetic nuclei, T_{1M} is the relaxation time of the coordinated nucleus, and τ_M is the mean residence time of the magnetic nuclei in the complex, T_{1os} is the outer sphere (non-coordination) contribution to the relaxation rate.

$$\frac{1}{T_{1p}} = \frac{pq}{T_{1M} + \tau_M} + 1/T_{1os} \qquad (14)$$

The effect of any paramagnetic ion on the relaxation rate is related to the distance (r) between the ion and the nucleus, as shown in equation 15 (51), where $f(\tau_c)$ is the correlation function for the nuclear interaction with the probe and C is a collection of constants that characterize the paramagnetic species.

$$\frac{1}{T_{1M}} = \frac{C}{r^6} \times f(\tau_c) \qquad (15)$$

τ_c is related to the correlation times characterizing the rotational motion of the separation vector between the paramagnetic center and nucleus studied, τ_r, the electron spin relaxation time, τ_s, and τ_M, by equation 16. In $Mn(H_2O)_6^{2+}$ τ_r^{-1} dominates τ_c^{-1} (52).

$$\frac{1}{\tau_c} = \frac{1}{\tau_r} + \frac{1}{\tau_s} + \frac{1}{\tau_M} \qquad (16)$$

If T_{1M} is much greater than τ_M (that is, the ligand exchange is very fast between the $Mn(H_2O)_6^{2+}$ complex and the bulk water solvent) and if $1/T_{1os}$ is small compared to $1/T_{1M}$ (almost always true for Mn^{2+} paramagnetic effects), then equation 14 becomes equation 17.

$$\frac{1}{T_{1p}} = \frac{pq}{T_{1M}} \qquad (17)$$

When small ligands interact with $Mn(H_2O)_6^{2+}$, displacing the coordinated water molecules, $1/T_{1p}$ for the water proton decreases (because this substitution decreases the q-value), but the process has little affect on $1/\tau_r$ since the motion of the complex is comparable to $Mn(H_2O)_6^{2+}$. However, when a larger ligand is added to a Mn^{2+}—water solution, a slight increase is observed in $1/T_{1p}$, even though there is a decrease in q because a larger decrease in $1/\tau_r$ due to hindered rotational degrees of freedom of Mn^{2+} in the Mn^{2+}-ligand complex perturbs the relaxation rate. An interaction of Mn^{2+} with a macromolecule is likely, therefore, to lead to a significant increase in $1/T_{1p}$, as a result of an increase in τ_r (the $Mn(H_2O)_6^{2+}$ rotational motion is decidedly slowed by complexation with the macromolecule). This effect is defined as enhancement, e_b, and is defined in equation 18, where the asterisk denotes enzyme being present, and where $1/T_1$ is the observed relaxation time with metal and $1/T_{1(o)}$ is the relaxation time in the absence of Mn^{2+}. e_b has also been observed to decrease (53, 54, 55) as the metal ion-macromolecular complex forms. This phenomenon has been explained either as a general increase in $1/\tau_c$ (for spin-proton dipolar interactions), i.e., a

$$e_b = \frac{(1/T_1^*) - (1/T_{1(o)}^*)}{1/T_1 - 1/T_{1(o)}} \qquad (18)$$

decrease in the access of water protons to the bound paramagnetic ion, or an increase in $1/\tau_r$ and thus τ_c^{-1} because there exists a state of less hindered rotation of water molecules in the environment of the bound paramagnetic species due to a more open enzymic site. In both cases, namely, a decrease in e_b or an increase in e_b, metal coordination is being monitored. e_b can be determined by titrating a fixed concentration of enzyme with various concentrations of metal (alternatively a fixed metal concentration can be titrated by varied enzyme) and observing the $1/T_1$. e_b then can be plotted versus substrate concentrations to produce a binding isotherm of the paramagnetic metal to enzyme (or substrate) yielding data on K_D.

e_T, the enhancement of $1/T_{1p}$ of the ternary complex over that of the binary complex, can also be studied by titrating the binary enzyme-metal ion complex with various concentrations of substrate and observing the effects on $1/T_1$. e_T can then give us provisional information as to the coordination scheme of the enzyme, substrate and metal complex. If e_T is more than e_b, a substrate bridge between enzyme and substrate exists (Type I enzyme); if e_T is less than e_b, a metal bridge is involved (Type II enzymes); while if e_T equals e_b, an enzyme bridge is in operation (Type III enzymes) (50). The possible coordination schemes are shown in Figure 3.

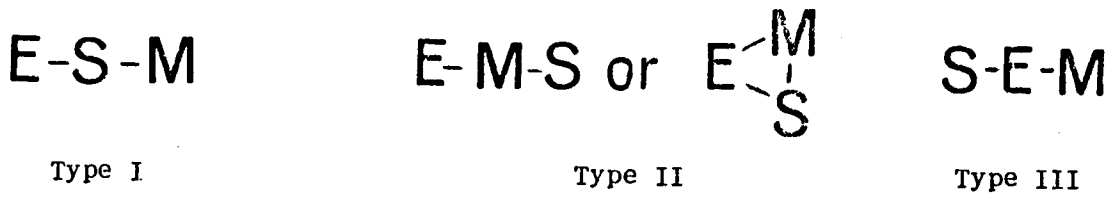

FIGURE 3. Possible coordination schemes for ternary complexes.

Measurement of enhancement provides a rapid and sensitive physical method which does not disturb the equilibrium under investigation and which can be used to determine values for K_D.

MATERIALS

Pressed Baker's yeast (Budweiser Brand) was obtained from Valenti Yeast, Inc. (Flushing, N.Y.), whereas whole blood was purchased from New York Blood Center (New York, N.Y.). Reagents supplied by Sigma Chemical Co. (St. Louis, Mo.) were PRPP (sodium salt), Adenosine triphosphate (sodium salt), Adenosine monophosphate (sodium salt), OMP (sodium salt), Dithiothreitol and Yeast Inorganic pyrophosphatase. Orotic acid was purchased from Calbiochem (LaSalle, Ca.) and 5-fluoroorotate was obtained from P. L. Biochemicals (Milwaukee, Wis.). The Blue Sepharose CL-6B, Sephadex G-25, -50, and -100, and the molecular weight standards for the SDS gel electrophoresis were supplied by Pharmicia Fine Chemicals (Piscataway, N.J.). Bio-Rad Laboratories (Richmond, Ca.) supplied the DEAE-cellulose anion exchange resin, Dowex AG-1X8 anion exchange resin (formate form), Chelex-100 cation exchange resin and the Biogel HT (hydroxylapatite). For the exchange studies, ^{32}[P]-labeled sodium pyrophosphate (7.167 Ci/mM), 6-^{14}[C]-labeled orotic acid hydrate (49 mCi/mM), uniformly labeled ^{14}[C]-adenosine monophosphate (0.01 mCi), Omnifluor, scintanalyzed toluene, triton X-100, and Brays solution were all purchased from New England Nuclear (Boston, Mass.). PEI cellulose F precoated TLC plastic sheets were obtained from Brinkmann, Inc. (Westbury, N.Y.). All other chemicals were reagent grade.

METHODS

Purification of OPRTase

All steps were performed at 4°C unless otherwise indicated. The purification procedure was adapted from Umezu, et. al. (4).

STEP #1. Autolysis: Ten pounds of pressed baker's yeast (Budweiser yeast, St. Louis, Mo.) were suspended in a mixture of potassium phosphate buffer (0.3 M, pH 8, 3 liters) and toluene (500 ml) and gently stirred for 4 hours at 30°C in a constant temperature bath. The pH was adjusted periodically to 8 by adding 5N KOH. After cooling overnight at 4°C the mixture separated into two phases; the aqueous lower phase was centrifuged in a Sorvall RC-2B refrigerated centrifuge for 20 minutes at 8,000 RPM (approximately 10,000 x g). The supernatant was filtered through a few layers of cheese cloth to remove fluffy lipid materials.

STEP #2. Ammonium Sulfate Fractionation: The autolysate (3.25 liters) was adjusted to pH 5 with 8N acetic acid with stirring in the presence of antifoaming octanol (1% v/v). To the acidified autolysate solid ammonium sulfate was added to obtain 50% saturation (313 grams ammonium sulfate per liter of autolysate). The addition was carried out over 5 hours with gentle stirring, and the solution was allowed to stand overnight to allow complete precipitation. The precipitate was collected by centrifugation (9,000 RPM, approximately 12,500 x g for 20 minutes) and dissolved in a minimum volume of Tris-HCl (25 mM, pH 8, about 1 liter). The solution was adjusted to pH 8 with 1N KOH and then dialyzed against 16 liters of Tris-HCl (10 mM, pH 8) overnight. The dialysate was centrifuged to remove precipitated debris (8,500 RPM, 20 minutes).

STEP #3. Ethanol Fractionation: The dialyzed ammonium sulfate fraction was made 50 mM in respect to $MnCl_2$ by adding 1 M $MnCl_2$. The solution was stirred for 30 minutes and centrifuged (8,500 RPM, 20 minutes) to remove nucleic acids. To each 750 ml portion of the supernatant, acetate buffer (2 M, pH 6, 100 ml) and orotate solution (10 mM, very insoluble, use heat, employed as a protective agent) were added, and the mixture was cooled to -2°C. To this mixture 95% ethanol (chilled overnight at -25°C) was slowly added, with stirring, to a concentration of 15% (v/v, 180 ml EtOH/1,000 ml solution). After stirring for 5 minutes at -15°C (temperature was maintained by a dry ice-acetone bath), the precipitate was removed by centrifugation (8,500 RPM, 10 minutes) at -15°C. The supernatant was then treated with additional ethanol to increase the concentration to 50% (820 ml EtOH/1,000 ml original solution). The precipitate collected by centrifugation at -15°C (8,500 RPM, 10 minutes) was dissolved in a minimum volume of Tris-HCl (25 mM, pH 8, 200 ml), stirred for 30 minutes and centrifuged. The precipitate was extracted once again with the same buffer and the combined extracts were dialyzed overnight against 16 liters of the same buffer.

STEP #4. Heat Treatment: The dialyzed ethanol fraction was made to 2 mM in $MgCl_2$ and 1 mM in orotate. Aliquots of 250-300 ml each in metal centrifuge cups were heated rapidly to 53°C in a constant temperature bath for 5 minutes, and then quickly cooled below 2°C in an ice-salt mixture. The denatured protein was removed by centrifugation (8,500 RPM, 20 minutes). In the purification procedure of Umezu, et. al. (4), a c_{γ} gel batchwise procedure should now be employed. This step was omitted from our workup after two attempts had shown no substantial increase in specific activity.

STEP #5. Sephadex G-100 Gel Chromatography: The heat treated supernatant was concentrated by an Amicon ultrafiltration unit (400 ml capacity) using a PM 10 membrane. A nitrogen pressure of 70 psi was employed until a concentration of approximately 100 mg/ml was obtained. The retentate (containing greater than 95% of the original activity) was divided into two portions and applied to a column (2.5 cm x 100 cm) of Sephadex G-100 equilibrated with 10 mM Tris-HCl (pH 8) buffer containing 1 mM orotate and 40 mM NaCl. Fractions of 15 ml were collected and those having a specific activity of 0.8 or greater were pooled.

STEP #6. DEAE-Cellulose Chromatography: The pooled G-100 fraction was dialyzed against 15 liters of potassium phosphate buffer (10 mM, pH 8) containing 1 mM orotate and then applied to a column (2.5 cm x 37 cm) of DEAE-cellulose equilibrated with the same buffer. The enzyme was eluted with a linear gradient between 750 ml each of 10 mM and 200 mM potassium phosphate buffer, pH 8, both containing 1 mM orotate. Fractions of 8 ml were collected and those with a specific activity greater than 4.5 were pooled. The enzyme activity eluted from DEAE-cellulose in two peaks, one major and one minor.

STEP #7. Biogel HT Hydroxyapatite Column: The major fraction from DEAE-cellulose was dialyzed against 10 liters of potassium phosphate buffer (pH 8, 10 mM) containing 1 mM orotate and then applied to a column (2 cm x 37 cm) of Biogel HT hydroxyapatite, previously equilibrated with the same buffer. The enzyme was eluted (in 8 ml fractions) with a linear gradient between 500 ml each of 10 mM and 200 mM phosphate buffer (pH 8), both containing 1 mM orotate. The active fractions were dialyzed against Tris-HCl buffer (pH 8, 10 mM).

The last hydroxyapatite step from Umezu, et. al. (4) was replaced with a Blue Sepharose column chromatography step (36). This step increased the yield of homogeneous enzyme by 41%.

STEP #8. Blue Sepharose Affinity Adsorbent Step: Twenty grams of Blue Sepharose CL-6B was washed in a sintered glass funnel with cold distilled water (200 ml per gram dry weight). The gel was then suspended in Tris-HCl buffer (pH 8, 10 mM) and poured into a column (2.5 cm x 25 cm) and equilibrated with the same buffer. The hydroxyapatite fraction was placed on the column and 6 ml fractions were collected. The column was washed with 10 mM Tris-HCl buffer (pH 8) until no more protein eluted. The enzyme was then eluted by washing the column with a solution of OMP (0.1 mM) in Tris-HCl buffer (pH 8, 10 mM). The purification steps are summarized in Table 2.

Spectroscopic Assays

Measurement of the initial velocities of the phosphoribosyl transfer reaction was carried out spectrophotometrically at 25°C using a Cary-15 recording spectrophotometer by methods previously described for fluoro-orotate (37) and orotate (4). The final concentrations of reactants in 1 ml of assay solution under conditions of substrate saturation were 100 μM PRPP, 300 μM orotate or fluoro-orotate, 1 mM $MgCl_2$, 50 mM Tris-HCl buffer (pH 8) and 2 x 10^{-4} mg of enzyme. Analogous concentrations were utilized in the product inhibition studies. Initial velocity measurements are calculated in units of μmoles OMP synthesized per minute. Measurements of the initial velocities of the pyrophosphorylysis of OMP were carried out at 25°C on the Cary-15 as described previously (4), with final saturating reactant concentrations in 1 ml of

Table II. Typical Purification of OPRTase from Baker's Yeast (10 lbs.)

Purification Step	Volume (ml)	Activity[(a)] (units)	Total Protein (mg)	Specific Activity (units/mg)	Purification (fold)	Recovery (%)
Autolysate	3,140	3,440	114,021	0.03	--	100
Ammonium Sulfate Fractionation (0 - 50%)	1,755	3,207[(b)]	49,023	0.065	2.2	93
Ethanol Fractionation (15 - 50%)	654	3,284	22,291	0.147	4.9	95
Heat Treatment (53°C, 5 min.)	760	2,857	13,499	0.212	7.1	83
Sephadex G-100	113	2,619	2,093	1.25	42	76
DEAE-cellulose	88	2,123	362	5.87	196	62
Biogel HT	45	1,631	36	45.3	1,510	47
Blue Sepharose	36	1,564	24	65.2	2,172	45.5

a) A unit of activity is defined as the amount of enzyme required to form 1 μmole of OMP in one minute.

b) OPRTase has been shown to be inhibited by ammonium sulfate (12).

assay mixture of 125 μM OMP, 2.5 mM pyrophosphate, 2 mM $MgCl_2$, 50 mM Tris-HCl (pH 8) and 2 x 10^{-4} mg of enzyme. For the product inhibition studies, the concentration of $MgCl_2$ was increased to 5 mM to insure that the divalent metal ion was in excess. Protein concentrations were determined according to the Lowry procedure (58).

Gel Electrophoresis

Disc electrophoresis was performed with 7.5% polyacrylamide gel preparations at room temperature (pH 8.9) by the method of Davis (59). Protein staining was accomplished overnight using 7% acetic acid containing 0.04% coomasie blue. Excess stain was removed from the gels by an overnight immersion in 7% acetic acid. Polyacrylamide gel electrophoresis in the presence of sodium dodecyl sulfate was performed by a modified (60) procedure of Shapiro, et. al. (61). Staining and destaining procedures similar to those described above were utilized. Standards used in SDS molecular weight determination were bovine serum albumin (M.W.-68,000), ovalumin (M.W.-43,000), pepsin (M.W.-35,000), α-chymotrypsinogen (M.W.-25,700), myoglobin (M.W.-17,200), and cytochrome C (M.W.-12,384).

Isotope Exchange

^{32}[P]-pyrophosphate exchange with PRPP was investigated in the following way. A reaction mixture, made up of 0.4 ml PRPP (10 mM), 0.1 ml PP_i (2.5 mM, 4.5 x 10^{-3} μCi), 0.45 Tris-HCl buffer (50 mM, pH 8), 0.02 ml $MgCl_2$ (0.1 M) and 5 μg of OPRTase, was allowed to incubate at room temperature for 15 minutes. Pyrophosphate solution (0.5 ml, 10 mM) was added at the end of this time period and the entire solution was applied to a Dowex-AG-1-X8 resin (formate form, 6.2 cm x 1.2 cm).

PRPP and pyrophosphate eluted separately through the use of a linear gradient regenerated by 250 ml H_2O and a 250 ml ammonium formate (1.5 M, pH 5) solution. Aliquots (1 ml) of fractions eluted by this gradient were added to Brays solution (10 ml) and counted using a Beckman LS-150 liquid scintillation counter. The locations of PRPP and PP_i in the eluent were established by methods described previously (62, 63). The above procedure was repeated with reaction mixtures containing 5 mM EDTA and a control containing no enzyme.

Studies of the exchange of ^{14}C-label between orotate and OMP were carried out in the following way. A reaction mixture made up of 0.3 ml OMP (1.25 mM, pH 7.6), 0.1 ml labeled orotate (3 mM, pH 7.5, 1.7×10^{-3} μCi), 1.6 ml Tris-HCl buffer (50 mM, pH 8), 0.01 ml $MgCl_2$ (0.1 M) and 4×10^{-4} mg of enzyme, was allowed to incubate at room temperature for 30 minutes. At the end of this time period, the enzyme was removed by heat treatment (100°C, 5 minutes) and the sample was placed on a Dowex AG-1-X8 column (formate form, 6.2 cm x 1.2 cm). Application of a solution of 0.625 M ammonium formate (pH 4.3) to this column readily eluted orotate followed by the elution of OMP. Fractions from this column were counted in a Nuclear-Chicago Liquid Scintillation counter by placing 1 ml aliquots in Brays solution (10 ml). The location of OMP and orotate in the eluent were located by measurement of sample absorptions at 267 nm and 295 nm, respectively. Control samples which contained no enzyme were run concurrently.

Isotopic Exchange Pattern

Exchange studies varying ^{14}C-labeled orotate at various fixed concentrations of OMP were performed by the method of Reyes (18, 64)

and Reyes and Guganig (65). Reaction mixtures contained 0.3 ml OMP (1.25 mM), varied concentrations of orotate (4 mM, 1.7 x 10^{-3} μCi), 0.025 ml $MgCl_2$ (0.1 M), and 5 μg of enzyme, made up to 1 ml with Tris-HCl buffer (50 mM, pH 8). Controls containing no enzyme and reaction mixtures containing 10mM EDTA with metal free enzyme were also run. All samples were incubated for 30 minutes at room temperature. The reaction was terminated by adding 0.01 ml of trichloroacetic acid (40% w/v). Each sample was spotted (5 x 4μl) in triplicate on Brinkmann PEI cellulose F precoated TLC plastic sheets. The sheets were developed in 0.2 M LiCl solution until the solvent front moved 16 cm. The sheets are air dried and the spots are visualized under 253 nM light. The spots are then cut out and placed into glass counting vials containing 1 ml of 0.1 M HCl/0.2 KCl solution. The vials are shaken gently for one hour at room temperature after which 10 ml of scintillation cocktail (toluene (1,000 ml) and triton X-100 (500 ml) added to 8.5 gms of Omnifluor) is added, and the samples are counted in a Beckmann LS-150 liquid scintillation counter. The above procedure completely resolves orotate from OMP (vide infra).

^{14}[C] -labeled PRPP Synthesis

Labeled PRPP was prepared in two steps. First, ^{14}[C] -labeled ribose-5-phosphate was obtained utilizing a procedure of Horecker (66) by heating AMP (0.2 gm containing uniformly labeled ^{14}[C] AMP, 0.01 mCi) in 1N HCl (2 ml) at 100°C for 30 minutes. The solution is cooled and the pH is adjusted to 6.5 with saturated $Ba(OH)_2$ (about 6 ml). The solution is centrifuged and 50 ml of ethanol (95%) was added. The resulting precipitate is washed with 2 ml of absolute ethanol and extracted with 3 x 2 ml of water. The combined extract is treated with

four volumes of ethanol and the precipitate is dried in vacuo. ^{14}[C] - labeled PRPP, utilizing the uniformly labeled ^{14}[C] - ribose, was biosynthesized via PRPP synthetase.

PRPP synthetase was isolated from human erythrocytes (67) through the DEAE-cellulose batch step. Human erythrocytes were separated from whole blood by centrifugation in the cold and were washed twice with 4 to 5 volumes of cold 0.9% NaCl. Hemolysates were prepared by adding 3 volumes of cold 1 mM EDTA solution to the washed packed erythrocytes. Endogenous nucleotides are removed by stirring the hemolysate with Norit-A charcoal (10 mg/ml) for 10 minutes, at the end of which, the stroma and charcoal are removed by centrifugation for 15 minutes at 12,000 x g. To the hemolysate was added 250 ml of a solution containing 0.3 mM ATP, 6 mM Mg^{+2} and 1 mM dithiothreitol. DEAE-cellulose was washed with 1 M dibasic sodium phosphate buffer and then distilled water until the pH of the wash water was 7.0. The DEAE-cellulose was resuspended as a slurry and 750 ml were added to the hemolysate solution, and the resulting mixture was stirred for one hour. The mixture was filtered through a buchner funnel, and the DEAE-cellulose pad was washed with 0.3 mM potassium phosphate buffer (pH 7) until the wash color was clear. The pad was then washed with one liter of 3 mM potassium phosphate buffer (pH 7) containing 50 mM KCl, 0.3 mM ATP, 6 mM Mg^{+2} and 1 mM dithiothreitol, and the wash is discarded. The DEAE-cellulose was then suspended in 300 ml of a 500 mM KCl solution containing 50 mM potassium phosphate buffer (pH 7.4), 0.3 mM ATP, 6 mM Mg^{+2} and 1 mM dithiothreitol and centrifuged at 2,000 x g for 15 minutes. The supernatant containing the partially purified PRPP synthetase is passed through cheese cloth and concentrated (Amicon ultrafiltration unit, PM 10 membrane, 70 psi) to about 100 ml.

^{14}[C]-PRPP was prepared according to the procedure of Flaks (68). 440 ml of 60 mM potassium phosphate buffer (pH 7.3), 16 ml of ribose-5-phosphate (0.1 M, containing ^{14}[C]-labeled ribose-5-phosphate), 12 ml of $MgCl_2$ (0.5 M) and 18 ml of 2-mercaptoethanol (1 M) were all added to a 2 liter Erlenmeyer flask and placed into a 37°C water bath. When the temperature reached 37°C, 24 ml of ATP (pH 7.5, 0.05 M), 30 ml of KF (1 M) and 20 ml of the PRPP synthetase were added and allowed to react for 30 minutes. The flask was then rapidly chilled to 10°C and 20 g of Norit were added. The mixture was immediately filtered through a celite pad (Johns-Manville) at 4°C and washed with 400 ml of ice cold water. The PRPP was isolated from the combined filtrate and washings by passing the solution through a Dowex 1 (formate form, 15 cm x 2.5 cm) column. The PRPP was eluted by a linear gradient of 500 ml each of water and 1.5 M ammonium formate (pH 5.0). The eluent (monitored for radioactivity by standard counting procedures) had two radioactive peaks; the first contained ribose-5-phosphate, while the second contained the PRPP. The PRPP was isolated by adding 10 ml of a 0.5 M $MgCl_2$ solution to the pooled second radioactive peak, followed by the addition of three volumes of ethanol (95%, -15°C). The mixture was allowed to stand overnight at -15°C while PRPP precipitated. The mixture was then centrifuged (2,000 x g, -15°C) and the precipitate was washed twice with ethanol (-15°C), followed by two washes, each with acetone and ether at room temperature. The magnesium salt was then dissolved in cold water and passed through a small Chelex-100 column to prepare the sodium salt of PRPP, which was stored at -76°C (yield approximately 8 μmoles PRPP, 37,000 CPM).

Isolation of $^{14}[C]$-labeled Ribosylated Enzyme Intermediate

4-8 μg of OPRTase were incubated with 0.3 ml $^{14}[C]$-labeled PRPP, 0.2 ml Tris-HCl buffer (50 mM, pH 8), 0.025 ml $MgCl_2$ (0.1 M), and 15 units of inorganic pyrophosphatase for 5 minutes at room temperature. The sample was immediately placed on a G-50 Sephadex column, equilibrated with Tris-HCl buffer (50 mM, pH 8, 2.5 mM $MgCl_2$), and eluted with the same buffer (3 ml fraction). One ml aliquots were counted in 10 ml of Brays solution as before. Controls containing to enzyme were also run.

Electron Spin Resonance (EPR)

Samples to be studied by this technique were prepared as follows. To solutions of orotate, OMP, PRPP, PP_i and enzyme in Tris-HCl (pH 8, 50 mM), all of which were previously eluted through Chelex-100 to remove metal contamination, were added various concentrations of $MnCl_2$. The final concentration of all of the solutions were 100 μM in respect to the substrates. The samples were placed in EPR cells specifically adapted for use with aqueous solutions and the EPR spectra were recorded using a Varian V 4500 X-band EPR at a frequency of 9.295 GHz and at a sweep field range of 3335 ± 500 gauss at room temperature.

Proton Resonance Relaxation (PRR)

Binary complexes were studied as follows. Solutions of $MnCl_2$ dissolved in Tris-HCl (pH 8, 50 mM) were titrated with various concentrations of metal free orotate, OMP, PP_i, PRPP and enzyme. The relaxation times of the binary complexes were determined on a CPS-2, 30 megaherz PRR instrument (Spin Lock Electronics Ltd., Ontario, Canada) at room temperature. The samplex were placed in 5 mM cellulose nitrate tubes and contained 0.1 ml each. Ternary complexes

containing fixed concentrations of $MnCl_2$ (250 μM), enzyme (76 μM in PRPP study, 4 μM in OMP study), and varied concentrations of PRPP and OMP were examined as well. Diamagnetic controls using equivalent concentrations of $MgCl_2$ in place of $MnCl_2$ were employed throughout these studies.

RESULTS

Enzyme Preparation

The orotate phosphoribosyltransferase, when isolated as described in the methods section, was homogeneous by the criteria of both polyacrylamide gel electrophoresis and SDS gel electrophoresis (see Figure 4 A & D). As shown in Figure 4C, one of the two protein bands observed after hydroxylapatite chromatography was eliminated from the preparation through the use of Blue Sepharose CL-6B chromatography, and a single active OPRTase band was observed even at high protein concentrations. A single band was observed also when SDS gel electrophoresis was employed (Figure 4D), and the molecular weight for this protein was determined to be $21,000 \pm 1,000$ (Figure 5). This is in contrast to the native protein preparation which had been shown by both molecular sieve chromatography and sedimentation velocity measurements to have a molecular weight of $40,000 \pm 2,000$ (Danyel, S., Shen, S., and Sloan, D. L., unpublished results). Thus the native OPRTase isolated from Budweiser Brand yeast has the same molecular weight as this enzyme, purified previously from another brand of yeast by Umezu, et. al. (4), and appears to be composed of two subunits of equal size. OPRTase in human erythrocytes also has been shown to contain two subunits, each having an approximate molecular weight of 13,000 (19).

Kinetic Analysis of Formation of Orotidine 5'-Phosphate

A pattern of parallel lines was observed when reciprocals (1/v) of the initial velocities of the phosphoribosyl transfer reaction were plotted versus $[PRPP]^{-1}$ at different fixed levels of orotate and at saturating levels of magnesium ion (Figure 6A). In separate experiments

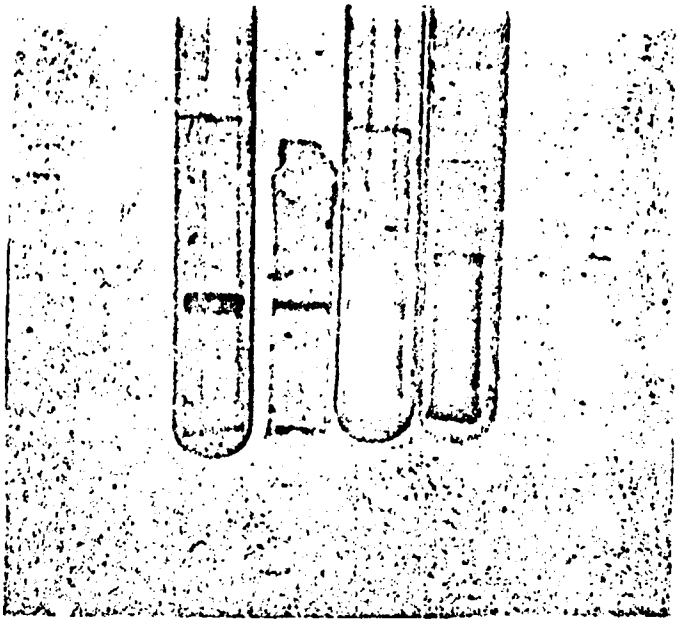

A B C D

Figure 4 . Polyacrylamide gels stained for protein as described in the methods section. A) 0.1 mg OPRTase after Blue Sepharose CL-6B column chromatography. B) 0.02 mg OPRTase after Blue Sepharose CL-6B column chromatography. C) 0.1 mg OPRTase after hydroxyapatite column chromatography. D) 0.05 mg OPRTase after Blue Sepharose CL-6B column chromatography in the presence of sodium dodecyl sulfate.

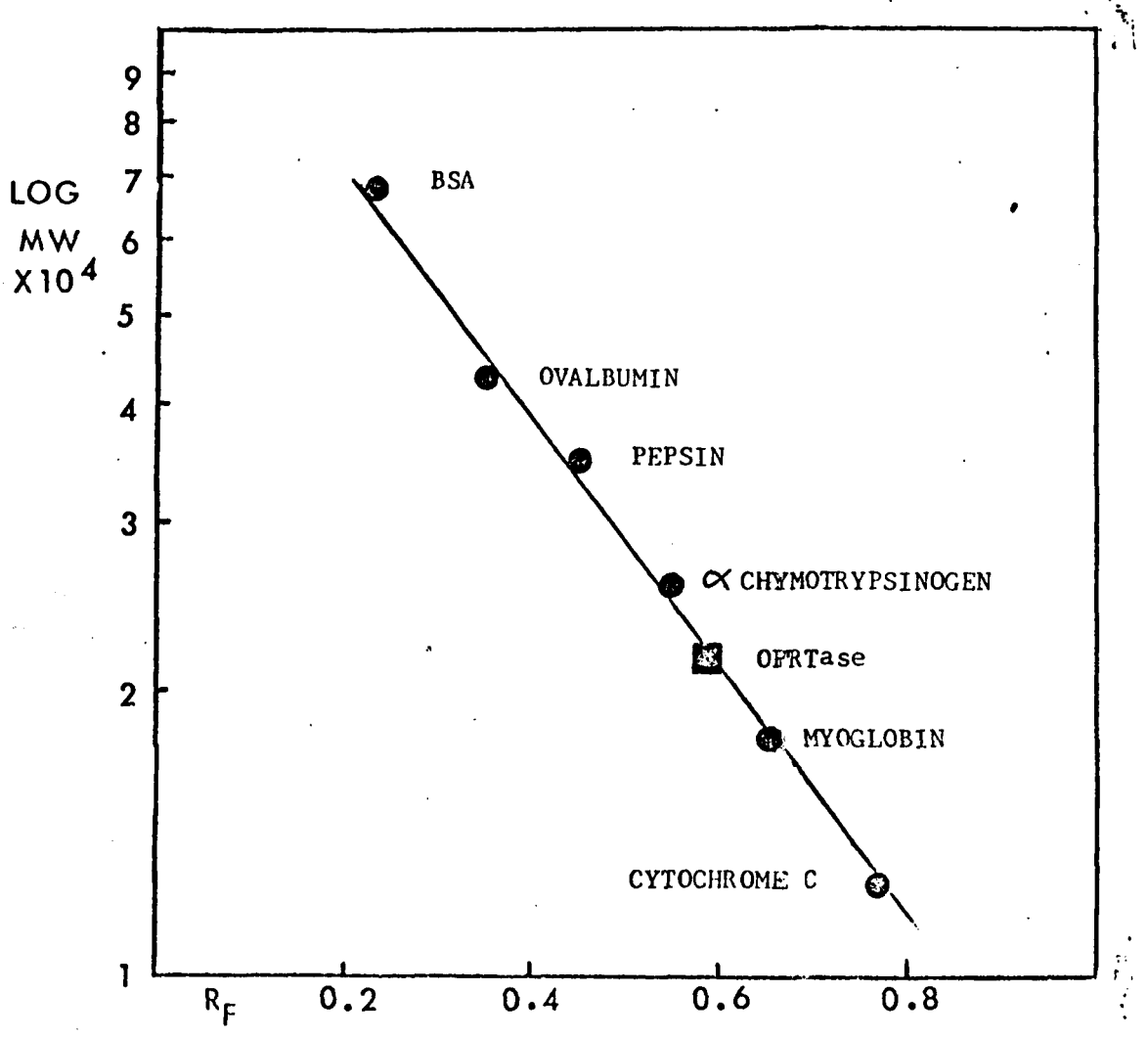

Figure 5 . Subunit molecular weight of OPRTase as determined by SDS gel electrophoresis.

Figure 6. Reciprocal initial velocity patterns for the formation of orotidine 5'-phosphate using the assay described in the methods section. (1/v units are μM OMP/min./mg protein for all plots.) A. Varied concentrations of PRPP in the presence of a 30-300 μM concentration range of orotate. B. Varied concentrations of orotate in the presence of a 20-100 μM concentration range of PRPP. C. Replots of the intercepts shown in 'A'. D. Replots of intercepts shown in 'B'.

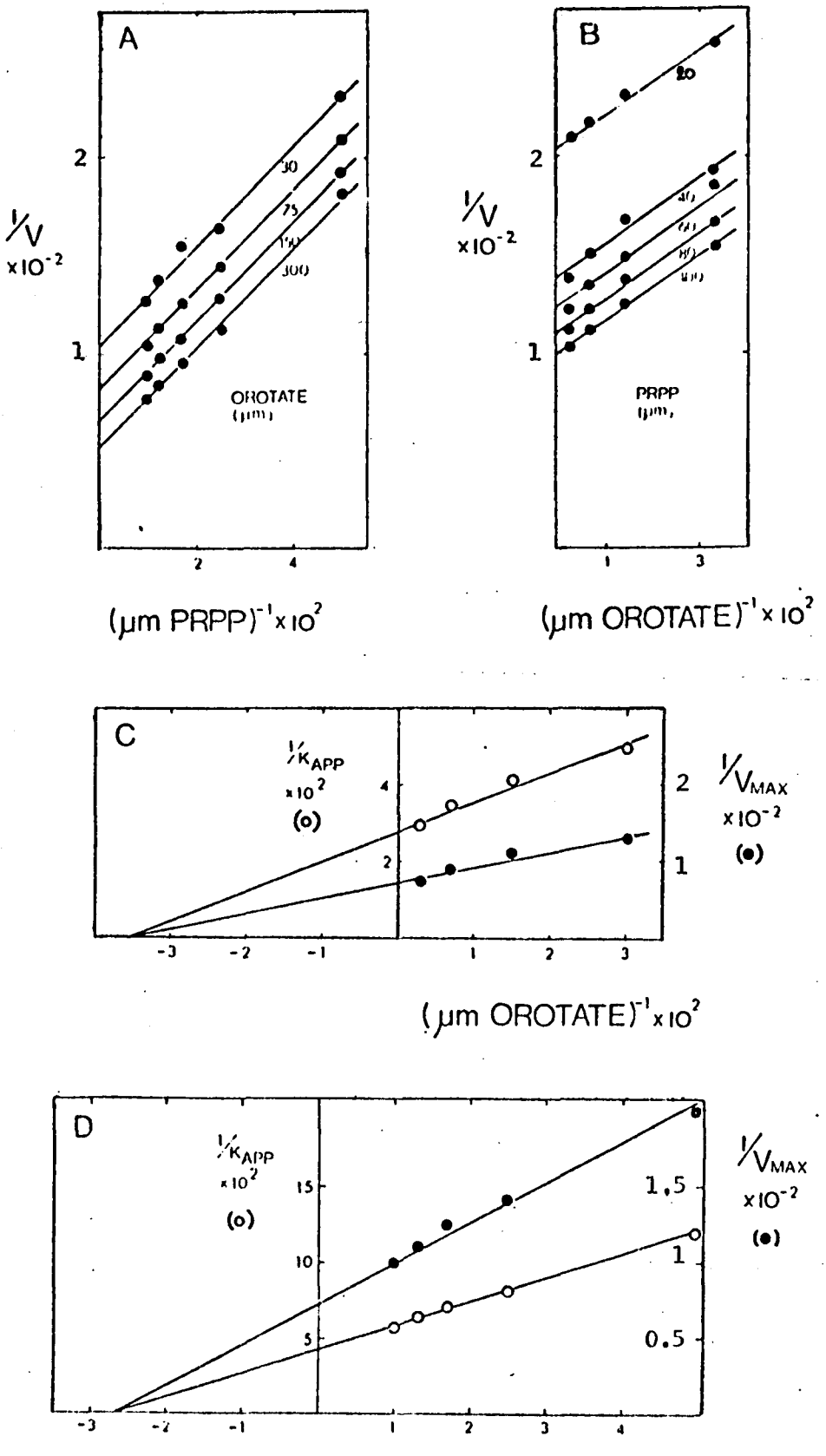
A
B
C
D
1/V x10⁻²
OROTATE (μm)
PRPP (μm)
(μm PRPP)⁻¹x10²
(μm OROTATE)⁻¹x10²
1/K_APP x10² (o)
1/V_MAX x10⁻² (●)

FIGURE 6.

the reciprocal initial velocity patterns of 1/v versus [orotate]$^{-1}$ were observed to be composed of parallel lines, as well (Figure 6D). Clearly, these results suggest a ping-pong type mechanism for formation of OMP from orotate as described by Cleland (69). Such a ping-pong mechanism can be illustrated by the half-reactions that are shown in equations 10 and 11. This mechanism assumes that PRPP is the first substrate to bind to the enzyme since it is the reactant which contains the group to be transferred.

Replots of the intercepts of Figures 6C and 6D were linear within the calculated error of each point (Figure 6C and 6D), and the K_m values for orotate and PRPP as determined by this graphical procedure are 22 ± 6 μM and 38 ± 8 μM, respectively. Umezu, et. al. (4) have reported a K_m value for orotate of 33 μM and a 62 μM value for PRPP. The discrepancy between these values and the ones presented in this paper may reflect, in part, the relative purity of the PRPP employed. The PRPP used by Umezu, et. al. (4) was 60% pure, whereas the commercial preparations used in our studies were at least 90% pure. It has been shown previously (38) that if impurities represent a significant fraction of the varied substrate, although the pattern of the reciprocal plots will not be affected (that is, parallel lines will remain parallel), and although there will be no changes in the 1/v-axis intercept, there will be an increase in the slopes of the plots, and therefore the apparent K_m values will all be greater than the actual values. A K_m value for PRPP similar to that found in this study has been reported for the OPRTase in Murine Leukemia P1534J (10). The data illustrated in Figure 6 was used to calculate a V_{max} value of 28.5 μM OMP/min / mg of protein.

Kinetic Analysis of Formation of 5-Fluoro-Orotidine 5'-Phosphate

Because 5-fluoro-orotate has been utilized extensively to assay for OPRTase activity in many tissues (57), a more limited study of the initial velocity patterns that result from the use of this substrate was undertaken in order to compare the resultant calculated kinetic parameters with those obtained for orotate. Using reactant concentrations similar to those employed in the orotate studies, a pattern of parallel reciprocal velocity lines was obtained (Figure 7A & B), suggesting a ping-pong mechanism for fluoro-orotidine 5'-phosphate, as well as secondary plots (Figure 7C and 7D) characterizing the K_m values for PRPP and F-orotate as 37 ± 7 μM and 24 ± 5 μM, respectively. These values are essentially the same as those determined from the orotate studies. Hence, it is likely that the modes of formation of F-OMP and OMP are analogous. In addition, a V_{max} value of 42 μM OMP/min /mg of protein was obtained for the formation of F-orotidine 5'-phosphate.

Initial Velocity Studies of the OMP-Pyrophosphorylase Reaction

As has been discussed previously, ordered bibi kinetic mechanisms involving substrates with very high enzymic binding affinities sometimes are characterized by reciprocal velocity patterns that appear to be composed of parallel lines. Seemingly parallel initial velocity patterns can also occur in rapid equilibrium random systems where the binding of one of the substrates inhibits the binding of the other. In both of these cases, product inhibition patterns can help distinguish these mechanisms from a ping-pong mechanism, but even this procedure is not foolproof. Thus, we

Figure 7. Reciprocal initial velocity patterns for the formation of 5-fluoro-orotidine 5'-phosphate using assay procedures described in the methods section. A. Varied concentrations of PRPP in the presence of a 15-300 μM concentration range of orotate. B. Varied concentrations of fluoro-orotate in the presence of a 20-100 μM concentration range of PRPP. C. Replots of the intercepts shown in 'A'. D. Replots of the intercepts shown in 'B'.

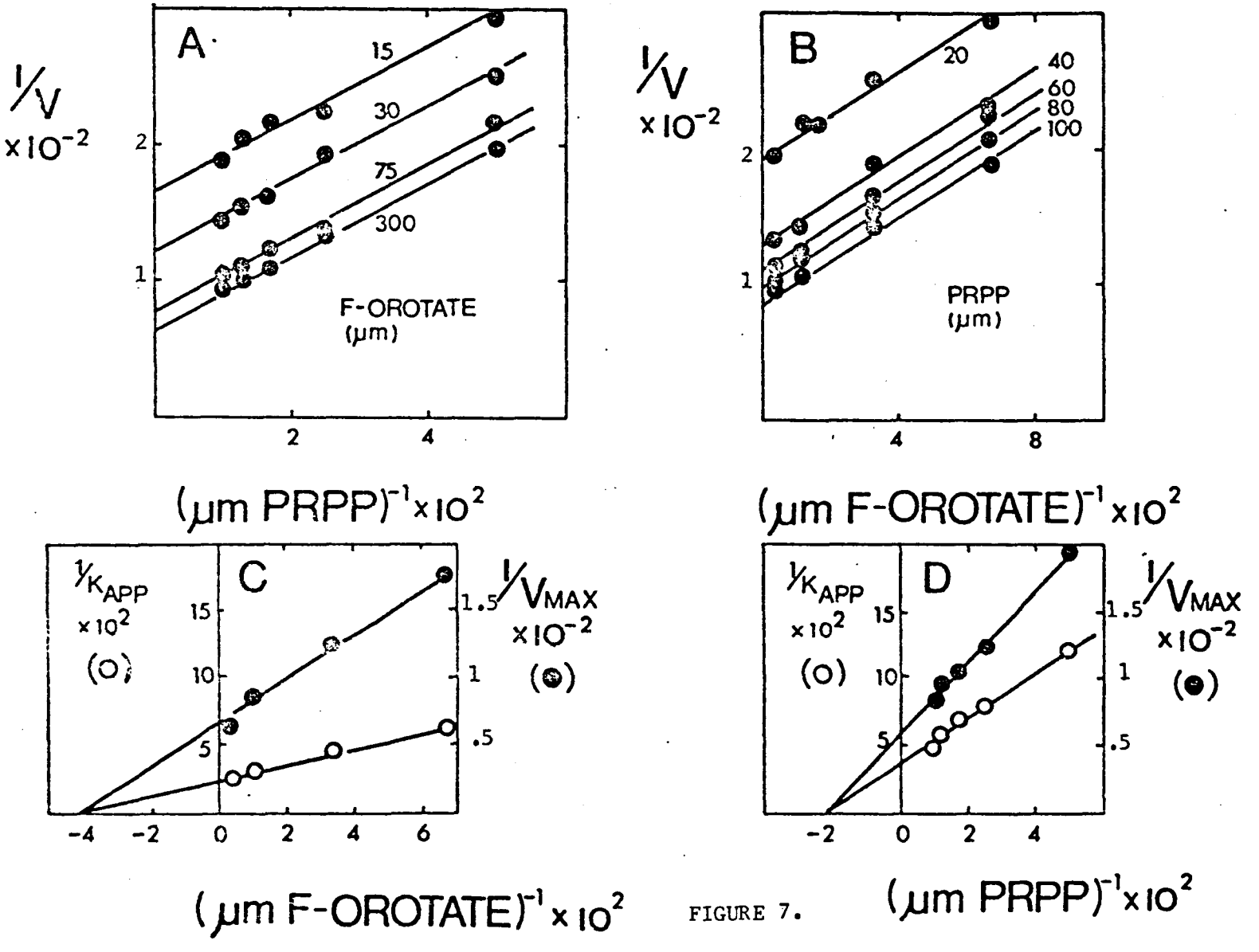
A
15
30
75
300
F-OROTATE (μm)
1/V x10⁻²
(μm PRPP)⁻¹x10²
B
20
40
60
80
100
PRPP (μm)
1/V x10⁻²
(μm F-OROTATE)⁻¹x10²
C
1/K_APP x10² (○)
1/V_MAX x10⁻² (●)
(μm F-OROTATE)⁻¹x10²
D
1/K_APP x10² (○)
1/V_MAX x10⁻² (●)
(μm PRPP)⁻¹x10²

FIGURE 7.

determined that studies of the reverse reaction, namely the formation of PRPP from OMP and PP_i, should be studied in detail by kinetic analysis in order to see if initial velocity patterns consistent with a ping-pong mechanism could be obtained. The observance of patterns of parallel lines for both reaction directions would render masked random or ordered bibi mechanisms unlikely. These studies were also initiated in order to obtain K_m values for PP_i and OMP. As shown in Figure 8 A and 8B, the reciprocal initial velocity patterns for the pyrophosphorylation of OMP in the presence of excess Mg^{2+} are indeed composed of parallel lines within the experimental error. The concentrations of OMP, Mg^{2+} and pyrophosphate required to generate these initial velocity patterns are higher than those required for studies of the product inhibition of the forward reaction (vide infra). The K_m values for PP_i and OMP were determined from replots (Figure 8C and 8D) to be 96 ± 6 μM and 8 ± 2 μM, respectively, and a V_{max} value of 31.3 μM OMP/min / mg of protein was calculated for the pyrophosphorylase activity. Umezu, et. al. (4) have determined the K_m values for these two substrates previously, and their value for OMP is analogous to ours. The K_m value of pyrophosphate as determined by these authors (4) is twice the value that is presented here. We can offer no explanation for this discrepancy.

Product Inhibition of Formation of Orotidine 5'-Phosphate

The interpretation of the kinetic mechanism as ping-pong and the characterization of PRPP as the first bound substrate is supported by the studies illustrated in Figures 9 and 10. As shown in Figure 9A, 9 B and 9C, the patterns of lines resulting from initial velocity

Figure 8. Reciprocal initial velocity patterns for the formation of PRPP. A. Varied pyrophosphate concentrations in the presence of a 13-125 μM concentration range of OMP. B. Varied OMP concentrations in the presence of a 250-2500 μM concentration range of pyrophosphate. C. Replots of the intercepts of 'A'. D. Replots of the intercepts of 'B'.

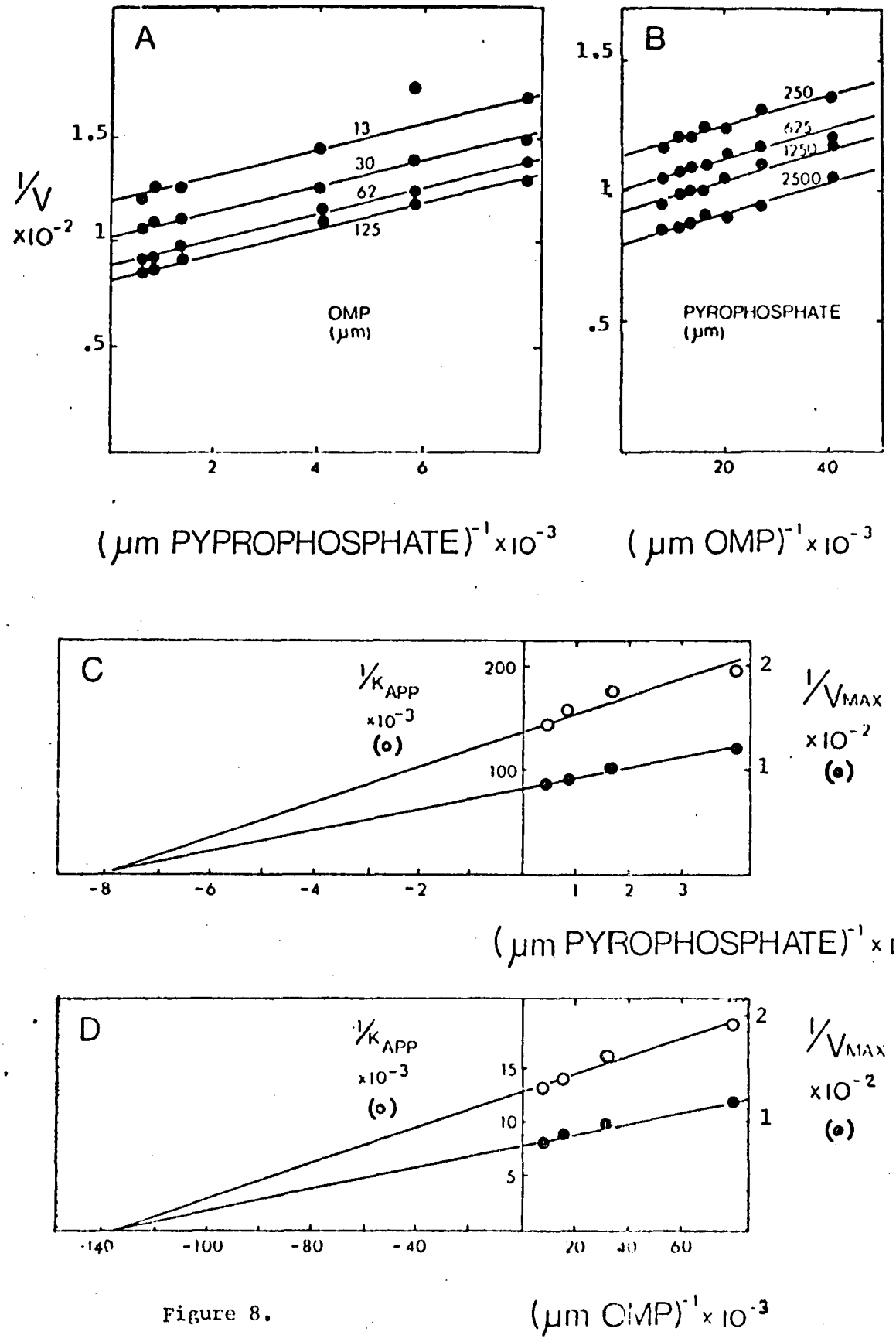
A
B
1/V
x10-2
1.5
1
.5
13
30
62
125
OMP
(μm)
250
625
1250
2500
PYROPHOSPHATE
(μm)
2
4
6
20
40
(μm PYPROPHOSPHATE)-1 x10-3
(μm OMP)-1 x10-3
C
1/KAPP
x10-3
(o)
200
100
2
1
1/VMAX
x10-2
(•)
-8
-6
-4
-2
1
2
3
(μm PYROPHOSPHATE)-1 x10-3
D
1/KAPP
x10-3
(o)
15
10
5
1/VMAX
x10-2
(•)
-140
-100
-80
-40
20
40
60
(μm OMP)-1 x10-3

Figure 8.

Figure 9. OMP product inhibition studies in the presence of fixed concentrations of orotate and varied concentrations of PRPP. A. 75 μM orotate. B. 150 μM orotate. C. 300 μM orotate.

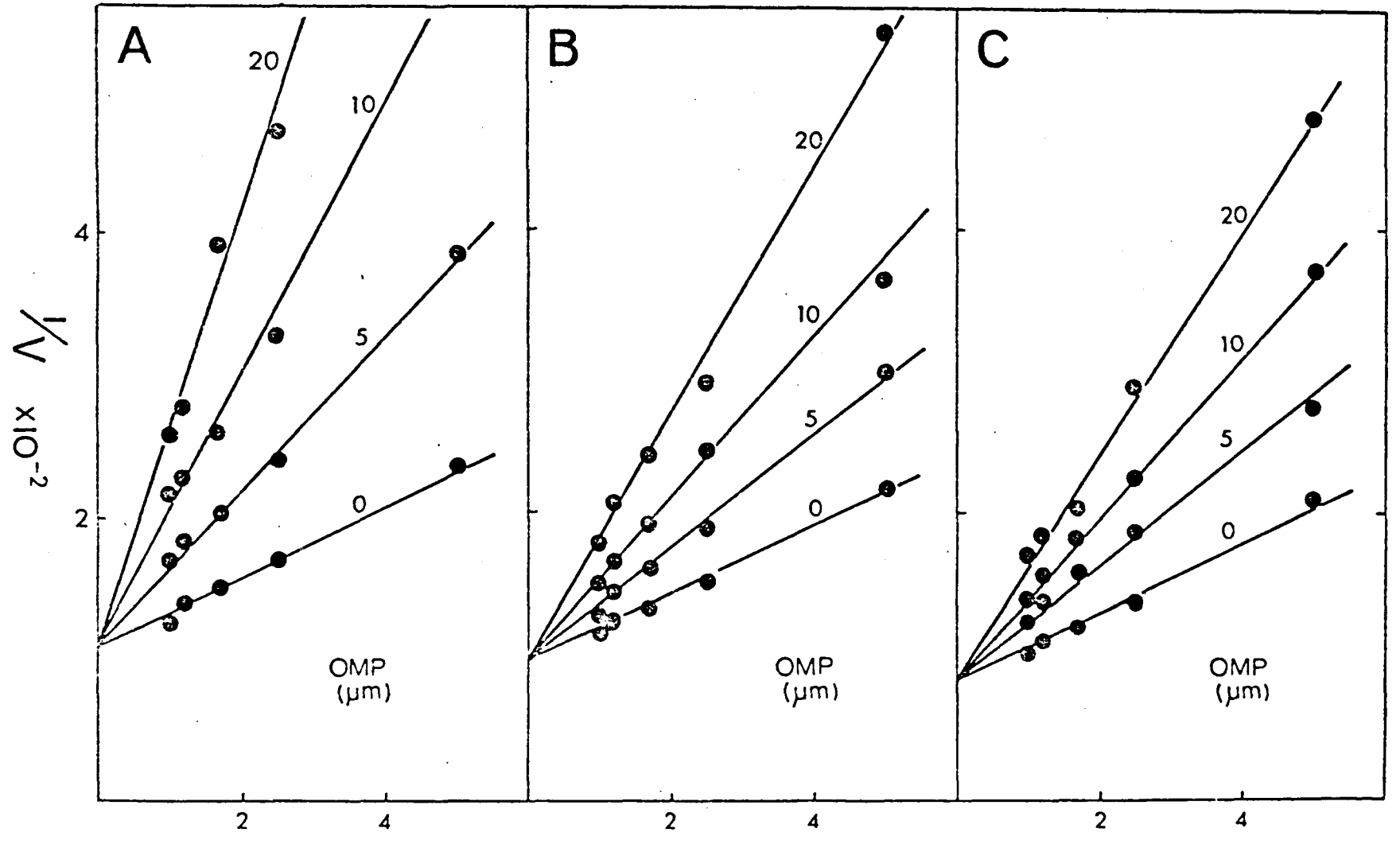

FIGURE 9.

studies at three fixed concentrations of orotate and varying concentrations of PRPP in the presence and absence of OMP intersect the y-axis at a common point. This competitive-type pattern confirms that PRPP is the first enzyme-bound substrate and that OMP is the last product released, and eliminates the possibility of a random mechanism for OPRTase. (This study utilizes a varied concentration of A(PRPP) at fixed, unsaturating levels of B(orotate) in the presence of product, Q(OMP), as explained previously in theory section, Table I.)

The product inhibition by PP_i of the phosphoribosyl transfer reaction, measured at three fixed unsaturating levels of orotate and varied concentrations of PRPP, characterize PP_i as a mixed-type inhibitor (Figure 10). This is fully consistent with a ping-pong mechanism in which pyrophosphate is the first product released and rules out a rapid equilibrium random bibi system. (This study varies the A(PRPP) concentration at fixed, unsaturating levels of B(orotate) in the presence of product, $P(PP_i)$.)

In addition, initial velocity studies at two fixed unsaturating concentrations of PRPP and varying concentrations of orotate in the presence of pyrophosphate display patterns of lines that intersect at a common point, the y-axis (Figure 11). This competitive-type pattern is clearly indicative of a ping-pong mechanism and rules out an ordered mechanism. (This study varies the concentration of B(orotate) at fixed, unsaturating levels of A(PRPP) in the presence of product, $P(PP_i)$.)

To confirm that the product inhibition studies clearly demonstrate a ping-pong mechanism, the analogous study (that is, varying $B(PP_i)$ at fixed, unsaturating A(OMP) in the presence of product, P(orotate)) was carried out for the pyrophosphorylase reaction. The pattern of reciprocal

Figure 10. Pyrophosphate product inhibition studies in the presence of fixed concentrations of orotate and varied concentrations of PRPP. A. 300 μM orotate. B. 150 μM orotate. C. 75 μM orotate.

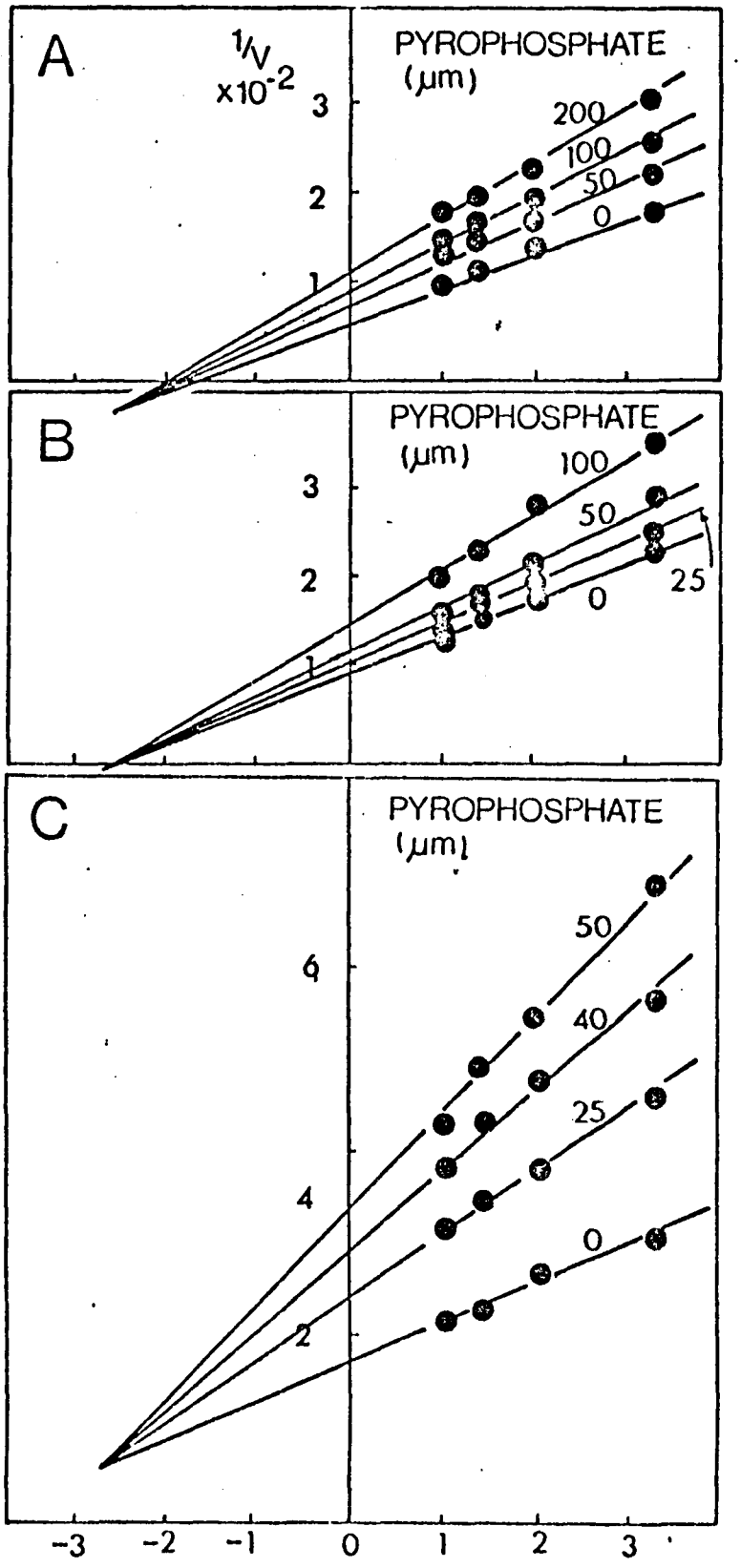
A
1/V
x10-2
PYROPHOSPHATE
(μm)
200
100
50
0
B
PYROPHOSPHATE
(μm)
100
50
25
0
C
PYROPHOSPHATE
(μm)
50
40
25
0
-3
-2
-1
0
1
2
3
(μm PRPP)-1 x 10^2

Figure 10.

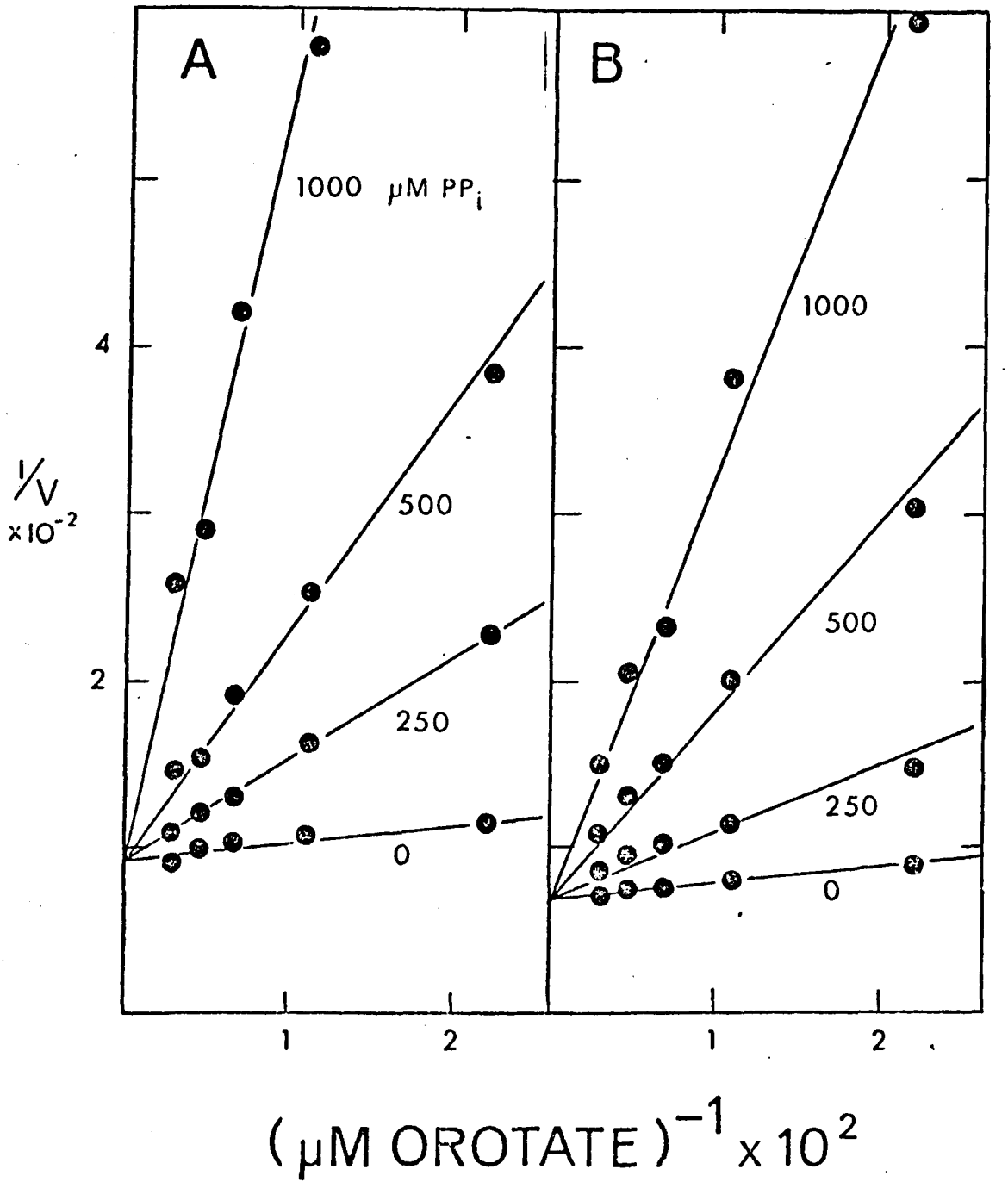

Figure 11. Pyrophosphate product inhibition studies in the presence of fixed concentrations of PRPP and varied concentrations of orotate. A. 50 μM PRPP. B. 100 μM PRPP.

velocity measurements versus $[PP_i]^{-1}$ at two fixed, unsaturating concentrations of OMP in the presence of varying, fixed concentrations of orotate are shown to be competitive, as well (Figure 12). These results are indeed consistent with the previous product inhibition studies of the phosphoribosyl transfer reaction and again preclude the possibility of an ordered mechanism for OPRTase. Apparent K_i values determined from replots of all the product inhibition studies described above are summarized in Table III, together with K_m and V_{max} values for OPRTase.

Isotopic Exchange

Because ping-pong kinetic mechanisms describe two somewhat independent half-reactions, proof that one half-reaction proceeds in the absence of substrates necessary for the second half-reaction, is proof of the ping-pong mechanism itself.

Studies of the formation of pyrophosphate from PRPP in the absence of orotate as illustrated in equation 10, were performed with $^{32}[P]$ - pyrophosphate. As shown in Figure 13, in the absence of enzyme, labeled pyrophosphate is not exchanged with the pyrophosphate moiety of PRPP, even though a significant number of the ribose-pyrophosphate bonds of PRPP are cleaved under these conditions (68). In contrast, addition of the enzyme in catalytic concentrations accomplishes this exchange (Figure 13B). When EDTA is added in slight excess of magnesium present the exchange of $^{32}[P]$ - pyrophosphate into PR $^{32}[P]$ -PP is reduced 65% (Figure 13A). This indicates that divalent metal is required for exchange to take place. Thus, the first half-reaction (equation 10) appears to proceed in the presence of metal but in the absence of orotate.

Figure 12. Orotate product inhibition studies in the presence of fixed concentrations of OMP and varied concentrations of pyrophosphate. A. 10 μM OMP. B. 100 μM OMP.

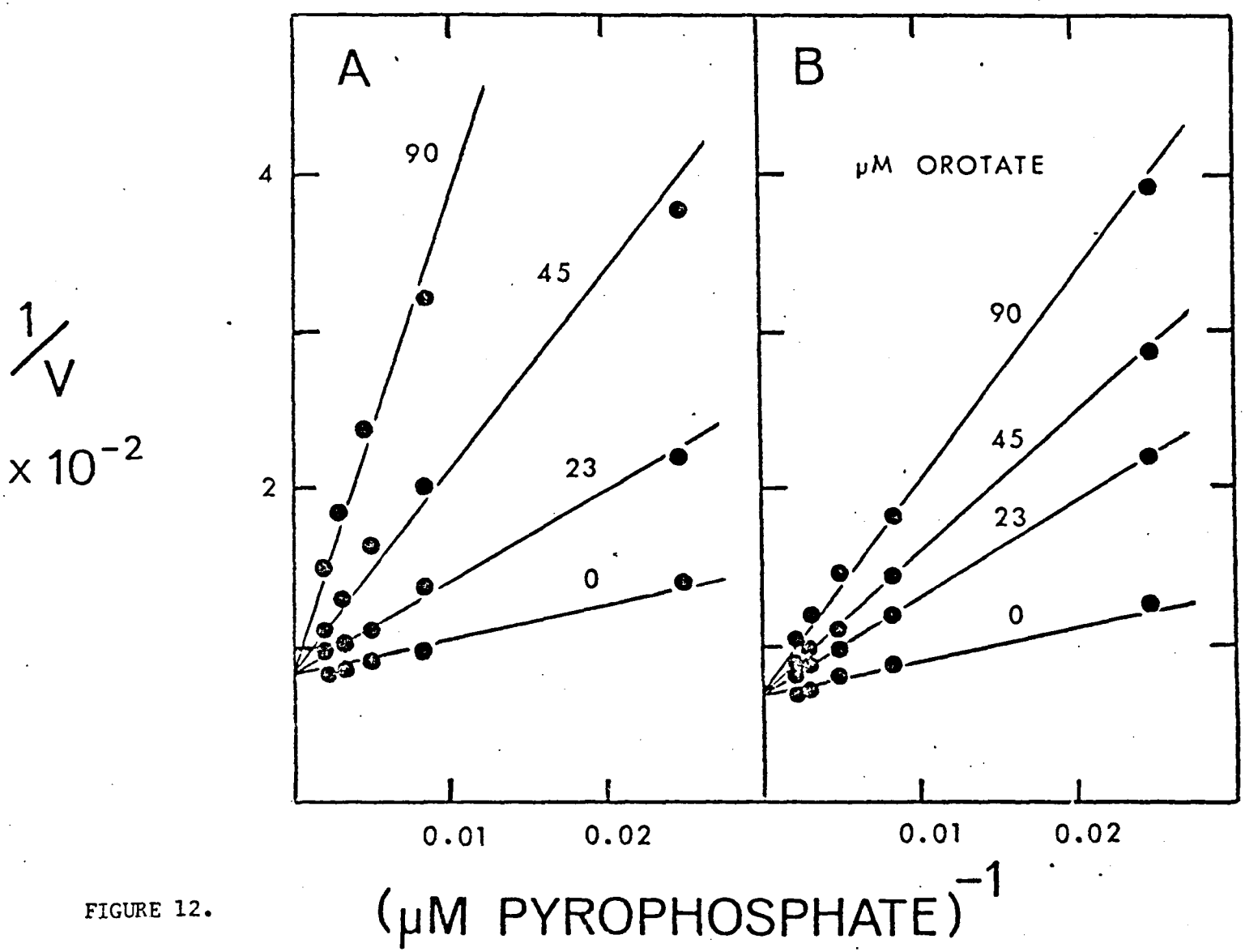

FIGURE 12.

Table III. Summary of Constants Characterizing the Reversible Reaction Catalyzed by Orotate Phosphoribosyltransferase from Yeast

Reactant	K_m (μM)	K_i (μM)	V_{max} (μM OMP/min/mg protein)
PRPP	38 ± 8	42 ± 5	--
OROTATE	22 ± 6	63 ± 12	--
PP_i	96 ± 6	202 ± 45	--
OMP	8 ± 2	9.8 ± 1	--
F-OROTATE	24 ± 5	24 ± 2	--
V_{max} forward	--	--	28.5
V_{max} reverse	--	--	31.3

Figure 13. Elution profiles of pyrophosphate and PRPP from Dowex AG-1-X8 anion exchange resin as described in the methods section. A. Elution of $^{32}[P]$ radioactivity after incubation of labeled pyrophosphate with cold PRPP in the presence of OPRTase from yeast and EDTA. B. Elution of radioactivity after incubation of labeled pyrophosphate with cold PRPP in the presence (closed circles) and absence (open circles) of OPRTase from yeast.

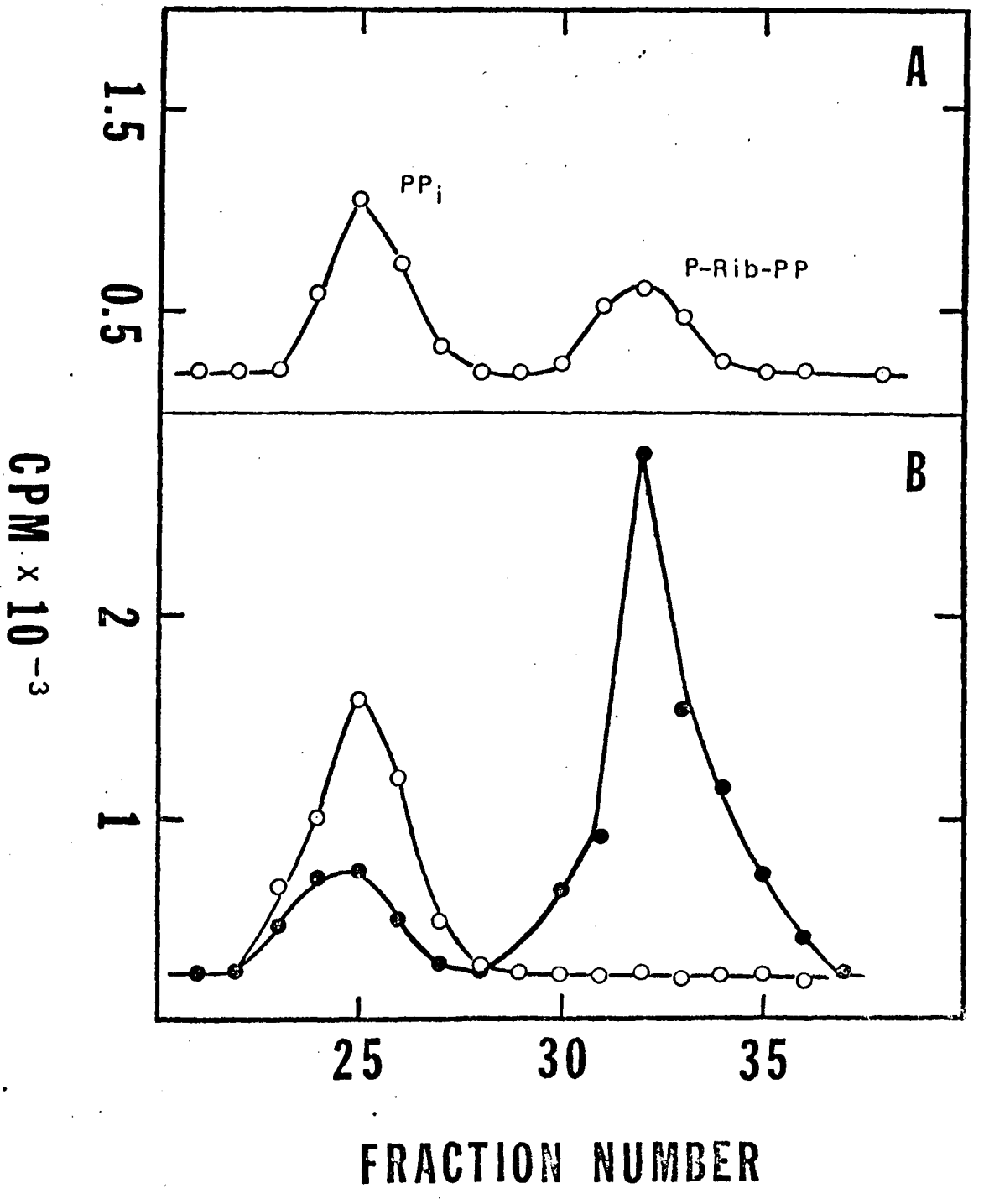

FIGURE 13.

As shown in Figure 14, the second half-reaction, namely, the interconversion of OMP to orotate, is catalyzed by OPRTase from yeast. Although the resolution of orotate from OMP on the Dowex resin is not complete in these experiments, there appears to be no exchange of label between orotate and OMP in the non-enzymatic sample as evidenced by the relatively symmetrical peak of radioactivity that elutes from the resin and that is maximal at the point where orotate is known to elute. In the presence of the enzyme, the peak is clearly unsymmetrical and substantial radioactivity is seen in the region where OMP elutes. Hence, studies of the exchange of label between substrate pairs in this reversible reaction establishes that the phosphoribosyl transfer reaction proceeds through a ping-pong mechanism, thus confirming the conclusions reached from kinetic analysis of the OPRTase reaction.

In an attempt to fully resolve the OMP and orotate from one another, a technique (64) which employs PEI cellulose TLC plates was utilized with great success. When OMP and orotate were cospotted on PEI cellulose plates and developed as described in the methods section, OMP migrated with an R_f of 0.02, whereas orotate displayed an R_f of 0.6. Thus, both orotate and OMP can be resolved completely from one another allowing a more detailed examination of this exchange reaction. In studies with varying concentrations of "cold" OMP and labeled orotate, up to an 18-fold increase of ^{14}[C] -label, incorporation into OMP was observed in the presence of catalytic amounts of enzyme. When the reaction mixture was eluted through Chelex-100 to remove divalent cations, and EDTA was added, only a 0.4-fold increase in label incorporation over the control was observed. This indicates, as was the case with the pyrophosphate-PRPP half-reaction, that the presence of divalent cations are necessary for exchange to occur.

Figure 14. Elution profiles of orotate and OMP from Dowex AG-1-X8 anion exchange resin as described in the methods section. A. The A_{295} absorbance profile for orotate (open circles) and the A_{267} absorbance profile for OMP (closed circles). B. Elution of $^{14}[C]$ radioactivity after incubation of labeled orotate with cold OMP in the presence (closed circles) and absence (open circles) of OPRTase from yeast.

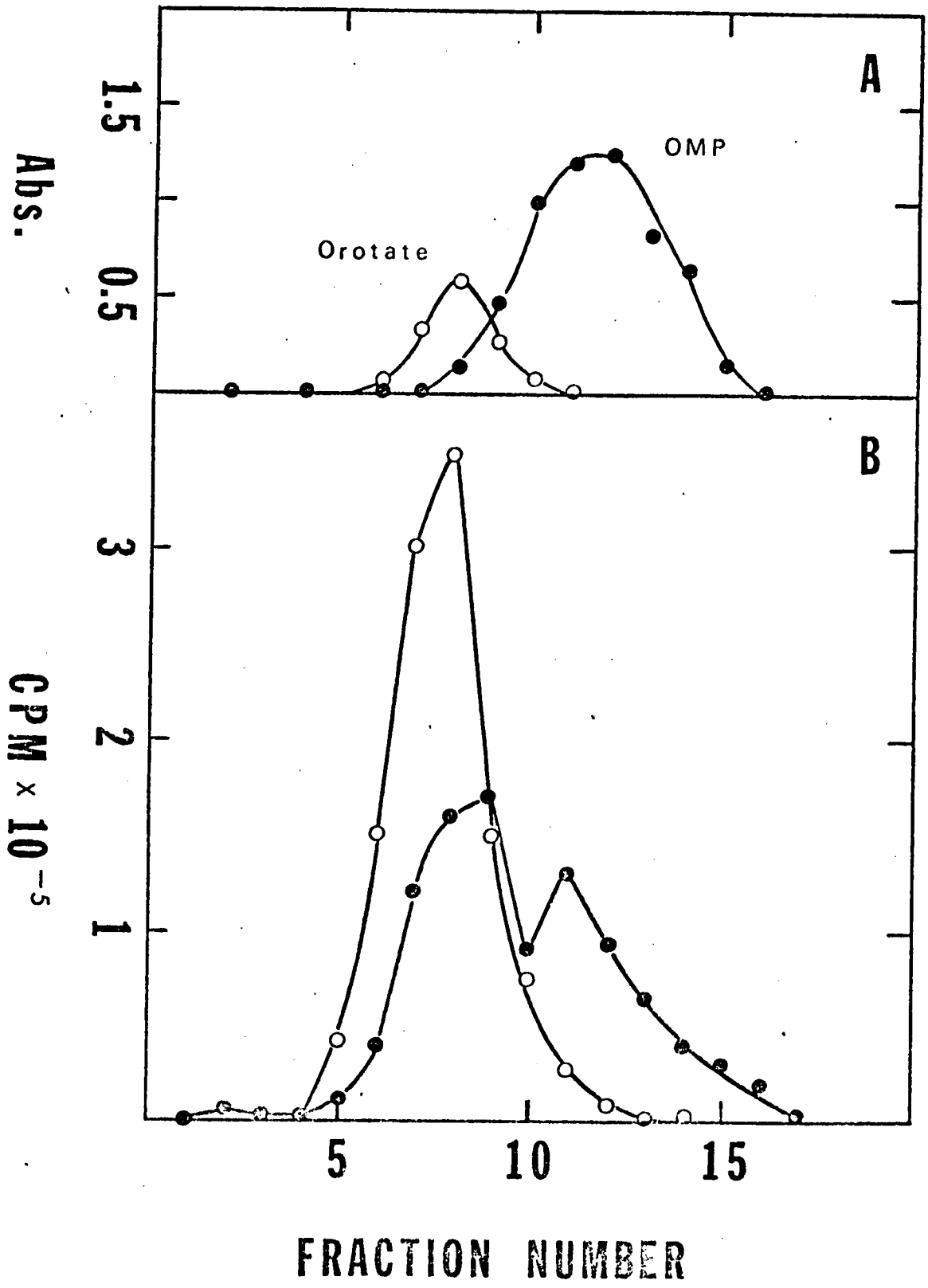

FIGURE 14.

Isotope Exchange Study

Reciprocal plot patterns for isotopic exchange of one of the half-reactions in a ping-pong system will display a set of parallel lines (44). However, substrate inhibition can be superimposed onto the predicted pattern at high concentrations of substrate causing a mixed-type inhibition to appear. We have observed these patterns with studies in which labeled orotate concentrations were varied at different fixed concentrations of OMP (Figure 15). As the concentration of OMP increased, slope and intercept effects were observed in the reciprocal exchange velocity pattern.

Isolation of the Ribose-Phosphate Enzyme Intermediate

^{14}[C] -PRPP was incubated with OPRTase in the presence of excess metal and inorganic pyrophosphatase. (This procedure was adapted from Bell and Koshland (70).) In a ping-pong mechanism the PRPP half-reaction will generate reversibly a phosphoribosylated enzyme and pyrophosphate (equation 10). By adding inorganic pyrophosphatase, which does not react with PRPP (68), to remove the pyrophosphate, we drive the reaction to the formation of enzyme intermediate. The labeled enzyme then can be separated from the unreacted labeled PRPP using molecular sieve chromatography. We employed both G-25 and G-50 column chromatography for this separation (Figure 16). The results were inconclusive; whereas a slight shift to higher molecular weight versus the control (^{14}[C] -PRPP alone) was seen for the enzyme ^{14}[C] -PRPP mixture elution pattern off of G-25, this shift did not occur for the elution through G-50. Further studies using labeled PRPP with a much higher specific activity and more enzyme may yield a clearer result. However,

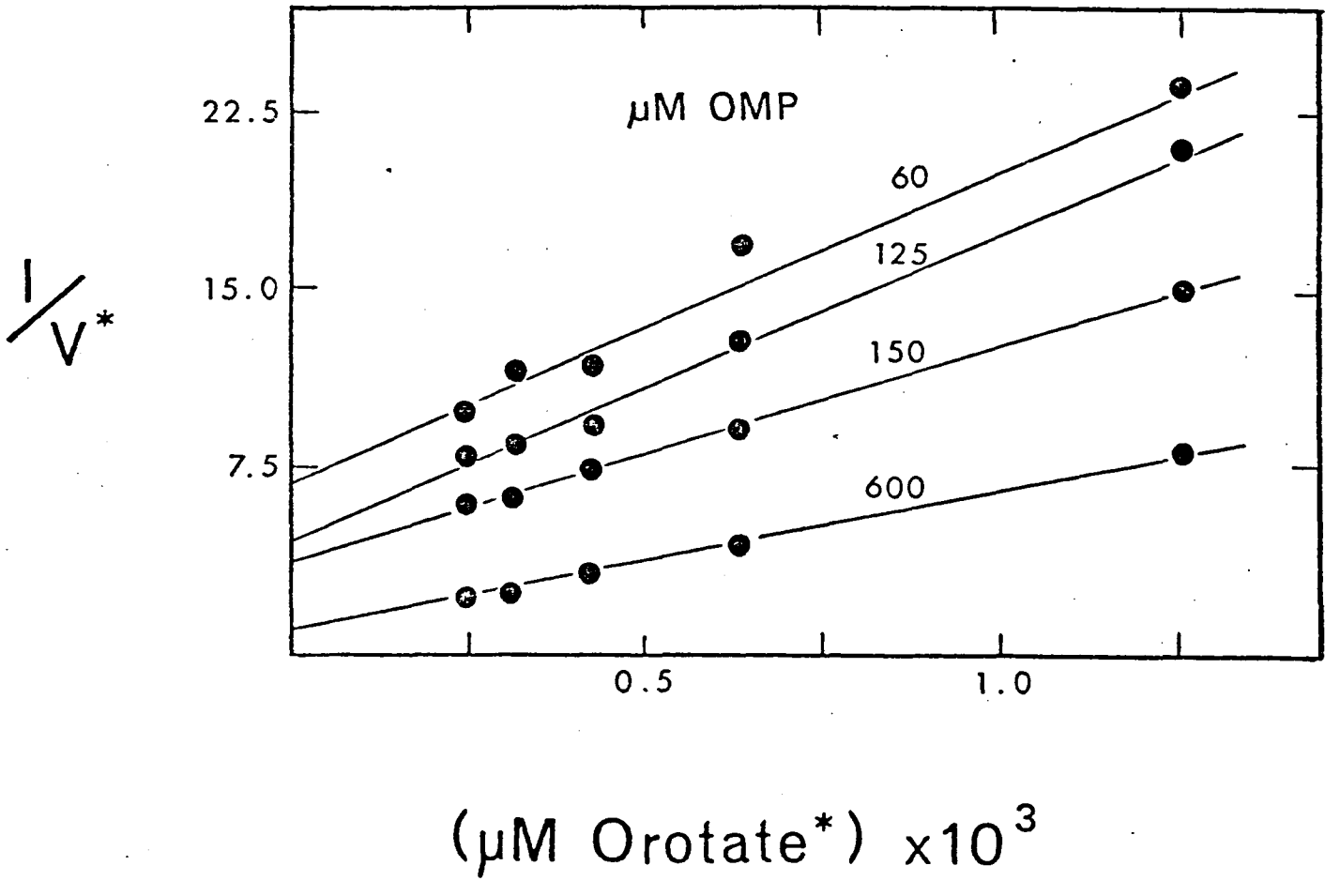

Figure 15. Isotopic exchange pattern between labeled orotate and unlabeled OMP. (v* units = cpm/min/ml of enzyme)

Figure 16. Isolation of phosphoribosylated enzyme intermediate. Elution profiles of: enzyme-^{14}[C]-PRPP incubation mixture (circles); and ^{14}[C]-PRPP control (squares), off of G-25 and G-50 columns.

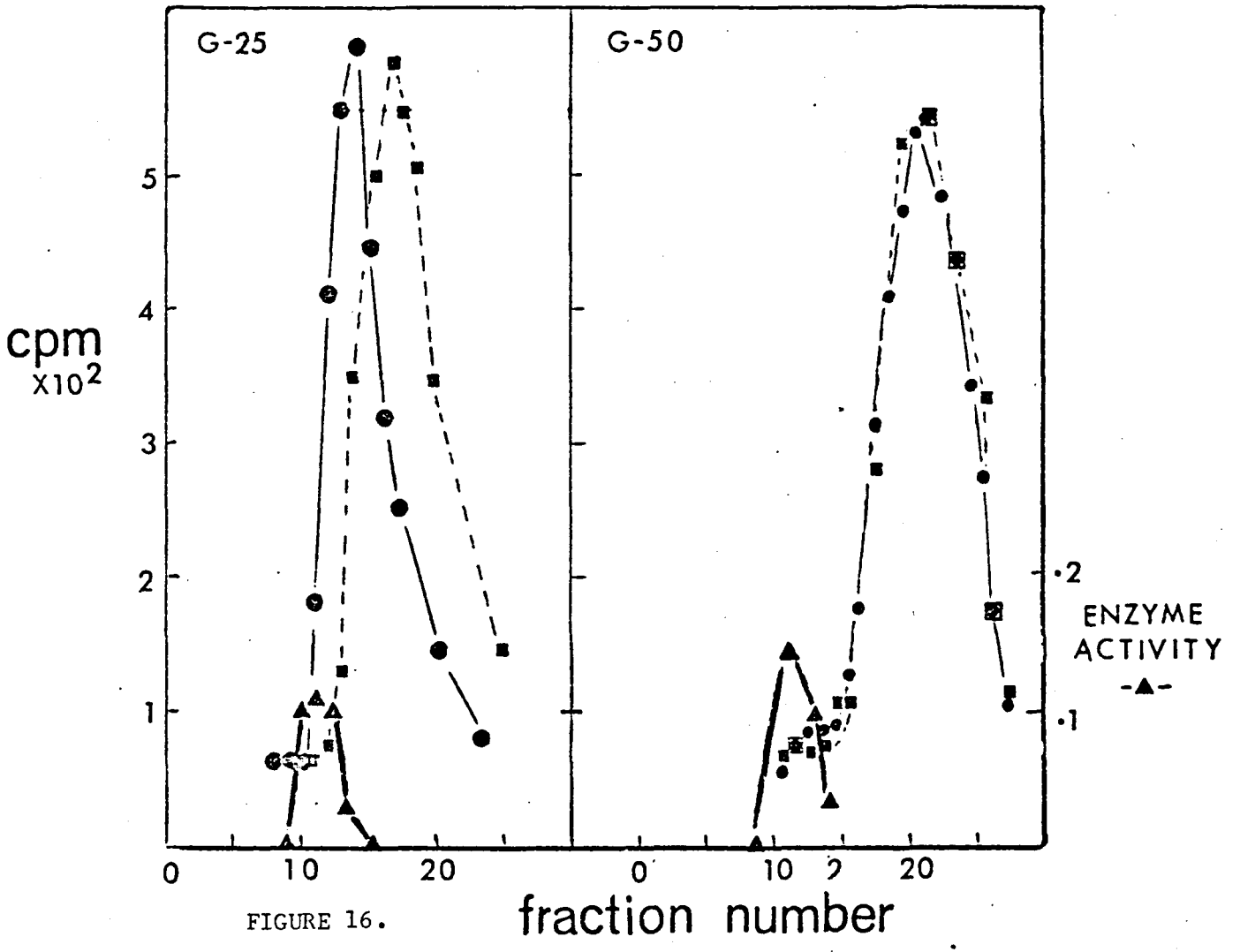
G-25
G-50
cpm
X10²
5
4
3
2
1
0
10
20
·2
·1
ENZYME
ACTIVITY
-▲-
fraction number

FIGURE 16.

the stability of the phosphoribose enzyme intermediate may be characterized if the intermediate can be trapped (see discussion section).

Electron Spin Resonance (EPR)

These studies provide only qualitative information about the binding of various substrates to Mn^{2+} because of a lack of instrument sensitivity in the detection of 100 μM Mn^{2+} in aqueous solutions. As has been discussed previously, the decrease in amplitude of the Mn^{2+} EPR signal upon addition of substrate indicates coordination of the substrate to the paramagnetic metal. When titrating solutions of orotate with various concentrations of Mn^{2+}, as discussed in the methods section, no decrease in amplitude of the Mn^{2+} EPR signal was detected, suggesting that Mn^{2+} did not form a complex with orotate at a Mn/orotate concentrations ratio of ≤ 2 in this study. Some OMP-Mn^{2+} coordination was exhibited (less than 5%) at higher concentrations of metal (90 μM and 100 μM). Titration of enzyme with a 0-500 μM concentration range of $MnCl_2$ showed a linear decrease in amplitude relative to a control in which H_2O was titrated with $MnCl_2$. This effect was not due to binding of metal, in our estimation, but is due to viscosity changes in the solution due to the presence of protein. Both PP_i and PRPP showed significant binding of Mn^{2+} as was evident from decreases in the amplitude of the Mn^{2+} signal relative to the control (Figure 17). Order of magnitude K_D values for PRPP and PP_i can be determined from this study and are on the order of 20-40 μM for both. (K_D values for PRPP and PP_i of 17 μM and 8 μM, respectively, have been recently determined by EPR (71).

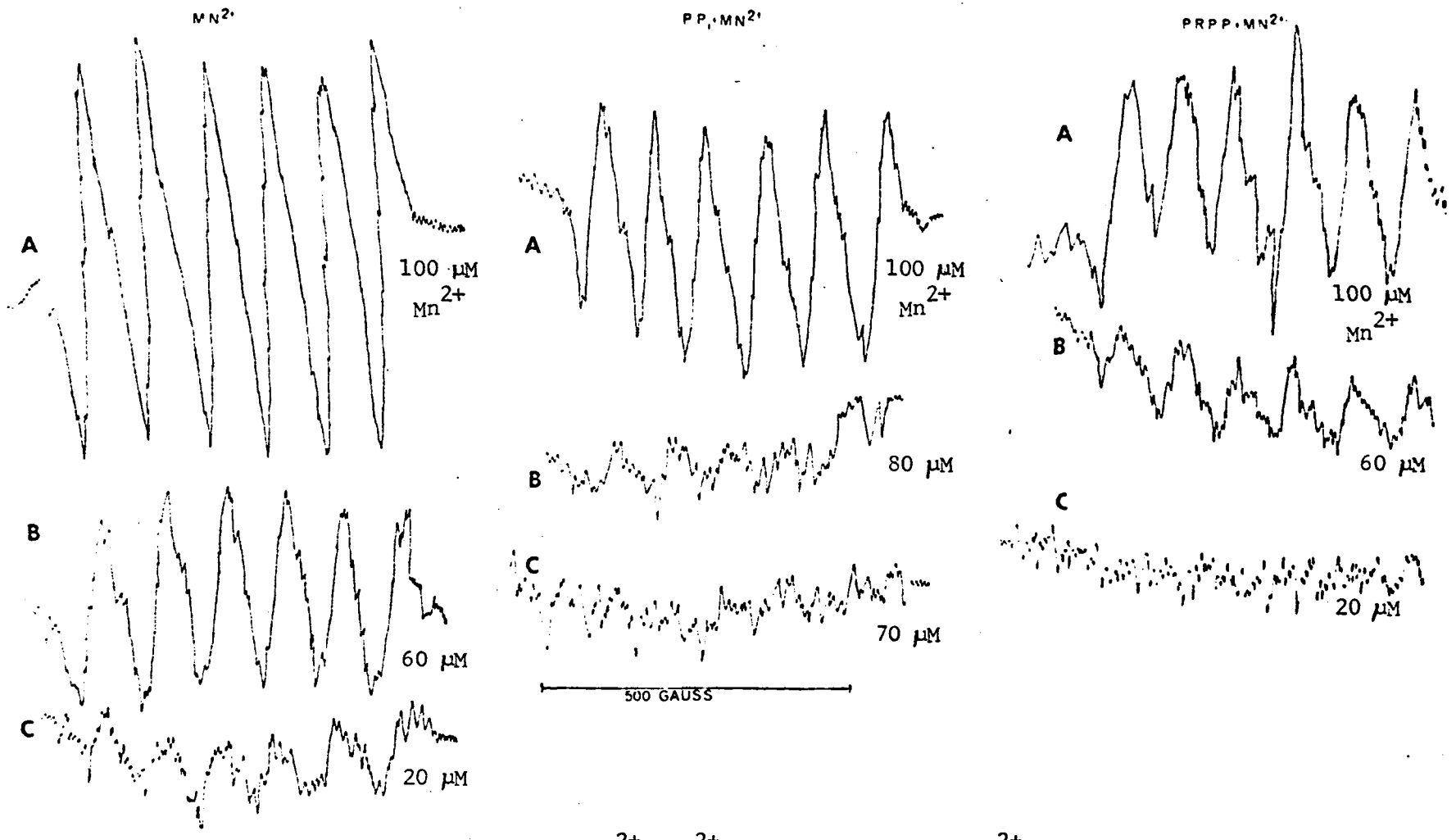

Figure 17. EPR spectra of Mn^{2+}, Mn^{2+}-PRPP complex, and Mn^{2+}-pyrophosphate complex. The concentration of PRPP and PP_i is each 100 μM at varied concentrations of Mn^{2+}.

Proton Resonance Relaxation (PRR)

Substrate binding of Mn^{2+} was determined quantitatively by preparing samples containing a fixed concentration of Mn^{2+} with various concentrations of the substrates and observing the effects on the longitudinal relaxation rate ($1/T_1$) of the water Mn^{2+} complex.

Both PP_i and orotate additions had no effect on $1/T_1$. From our EPR studies we had not observed effects consistent with the binding of orotate to Mn^{2+} and little if any perturbation of the Mn^{2+}-H_2O $1/T_1$ was expected. However, as PP_i was observed to bind to Mn^{2+} using EPR, the absence of an effect must be due to the small size of the PP_i-Mn^{2+} complex. Such a PP_i-Mn^{2+}-H_2O complex might not be expected to be different from a Mn^{2+}-water complex in respect to their molecular motions or tumbling times (τ_r), and thus an effect on $1/T_1$ would not be observed. Although the motion at room temperature for the Mn^{2+}-PP_i complex could be the same in both the EPR and PRR experiments, the frequency associated with these resonance techniques are very different.

Binary complexes of PRPP, OMP and OPRTase with Mn^{2+} were detected using the PRR technique. Mn^{2+} clearly binds to the enzyme but displays cooperativity in its binding, as is evidenced from the sigmoidal curve of the binding isotherm, as well as the Scatchard plot generated from these data (Figure 18A and 18B). From this observation we can project that Mn^{2+} may have two roles in the enzyme mechanism, acting as an allosteric effector of the enzyme and being part of the PRPP-metal substrate complex (the true substrate). When enhancement, ϵ^*, is plotted versus Mn^{2+} concentration for the enzyme-Mn^{2+} complex (Figure 19B), a decrease in enhancement is evident. Such decreases in enhancement due to the binding of paramagnetic species have also been observed with alcohol

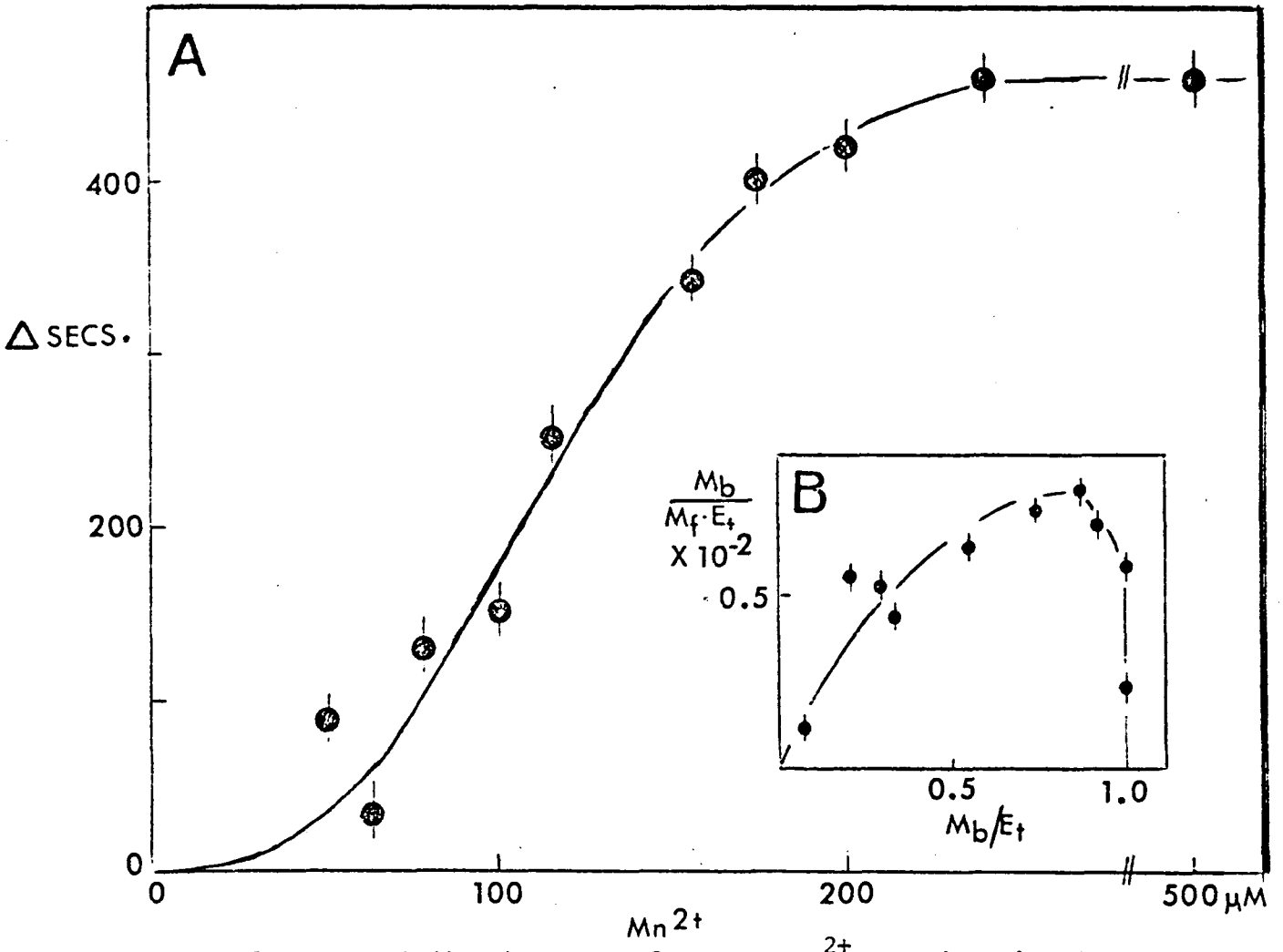

Figure 18. A. Binding isotherm of OPRTase-Mn^{2+} PRR titration (Δ sec. = change in T_1). B. Scatchard plot of data in A.

Figure 19. PRR titration studies measuring the enhancement (e^*) of $1/T_1$ of water. A. PRPP titration of Mn^{2+}. B. Mn^{2+} titration of enzyme. C. PRPP titration of Mn^{2+}-enzyme complex.

FIGURE 19.

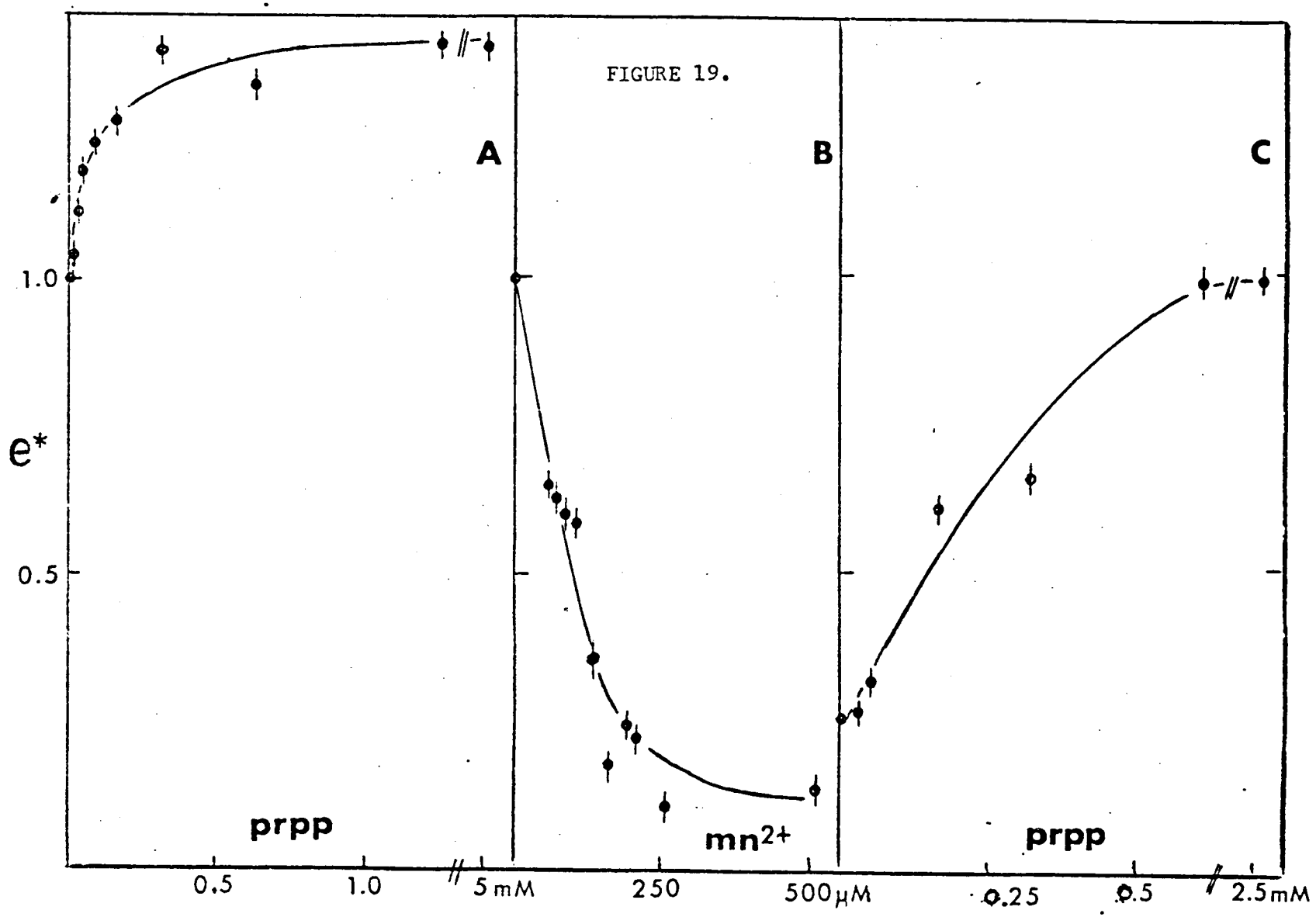

dehydrogenase (54) and sheep kidney Na^+/K^+ ATPase (55).

PRPP forms a binary complex with Mn^{2+} as is shown in Figure 19A. From this plot a K_D value of 40 μM for the PRPP-Mn^{2+} complex emerges. This value is in fair agreement with the value obtained from the EPR studies. The OMP-Mn^{2+} complex exhibits a much higher K_D value (Figure 20A) of approximately 1.5 mM.

When the substrate-enzyme-Mn^{2+} ternary complexes are studied by titration of a constant enzyme-metal concentration with various concentrations of substrate, we observe increases in enhancement (Figures 19C and 20C). This is true for both the PRPP and OMP ternary complexes (Figures 19 and 20, respectively). These effects are suggestive of formation of ternary complexes and are due to immobilization of water protons near the enzyme-bound metal. However, the study of the nature of the ternary complexes are complicated by the ping-pong mechanism which forces us to consider the on-off rates of the products as well as the initial substrates.

In summary, from the PRR data we can infer that the OMP-Mn^{2+} complex is not the true kinetic substrate for the enzyme, as the K_m for OMP is 8 μM and the K_D for OMP-Mn^{2+} is 1.5 mM. PRPP-Mn^{2+}, on the other hand, is probably the true substrate for the enzyme since the K_D of 40 μM is in close agreement with the K_m. Although ternary complexes of OMP-enzyme-metal and PRPP-enzyme-metal were detected, no clear picture as to the nature of these complexes can be deduced from these studies.

Figure 20. PRR titration studies measuring the enhancement (e^*) of $1/T_1$ of water. A. OMP titration of Mn^{2+}. B. Mn^{2+} titration of enzyme. C. PRPP titration of Mn^{2+}-enzyme complex.

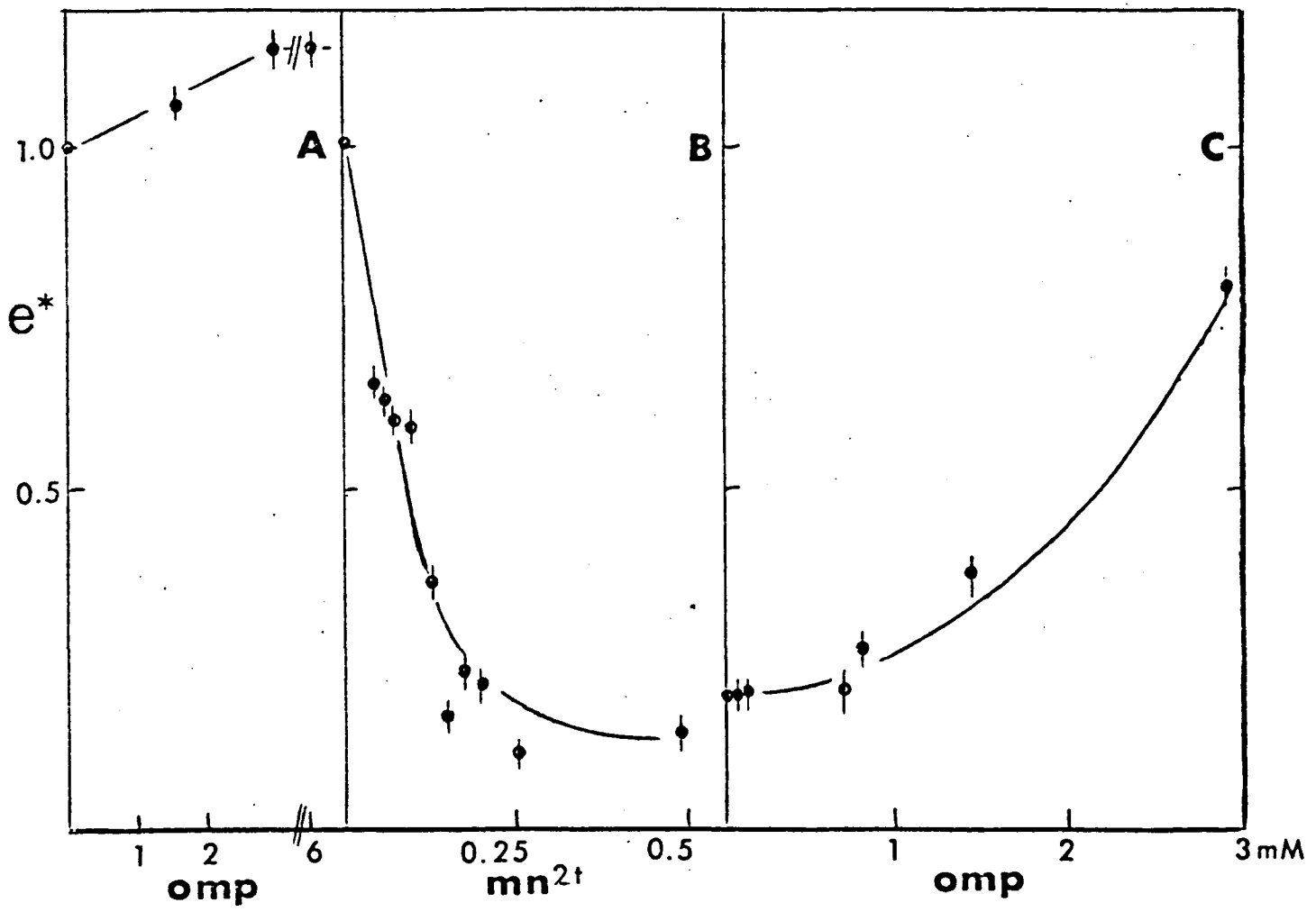

FIGURE 20.

DISCUSSION

There have been other instances where a phosphoribosyltransferase has been suggested as proceeding through the use of a ping-pong mechanism. Crude preparations of quinolate phosphoribosyltransferase (PRTase) exhibited parallel initial velocity patterns which proved to be clearly intersecting with purer preparations (72). Adenosine PRTase also showed parallel initial velocity patterns but product inhibition studies and isotope exchange experiments established the mechanism as being ordered (73). Bell and Koshland (70) proposed a ping-pong mechanism for ATP-phosphoribosyltransferase as a result of their apparent isolation of a labeled enzyme-ribose 5'-phosphate intermediate from ^{14}[C] -PRPP. Later studies by Parsons and his colleagues demonstrated this labeled intermediate to be an enzyme-product complex (74, 75) and determined by kinetic analysis that the mechanism of catalysis utilized by ATP-phosphoribosyltransferase from Salmonella typhimurium is an ordered bibi mechanism (76, 77). A ping-pong kinetic mechanism has also been implicated in the action of hypoxanthine-guanine phosphoribosyltransferase from human erythrocytes because parallel reciprocal initial velocity lines were obtained (73). While product inhibition studies of hypoxanthine-guanine PRTase seemed to indicate that an ordered mechanism was in operation and, therefore, the parallel patterns were a result of a K_{ia} that was much smaller than the K_{mA} (78). Subsequent work on pure preparations of human hypoxanthine-guanine PRTase (39) has shown that the K_{ia} to K_{mA} ratio was greater than 0.1 and, therefore, deviations from parallel lines should be detectable, and yet a graphical analysis still yielded parallel initial velocity

patterns. Moreover, an ordered mechanism would not explain the initial burst of IMP synthesis observed upon addition of hypoxanthine to enzyme which was previously incubated with PRPP. Krenitsky, et. al. (39) reconciled the data and showed that at the optimum metal concentration a ping-pong mechanism is in operation while at low metal concentrations (50 μM) a sequential mechanism existed. Thus, the interpretation of our characterization of the reciprocal initial velocity patterns for OPRTase from yeast as being composed of parallel lines was approached with caution. However, by two other criteria, namely, product inhibition patterns and studies of isotopic exchange, a bibi ping-pong mechanism for OPRTase from yeast was confirmed (in the presence of excess metal ion).

From the PRR and EPR data, it appears that the binary complexes of magnesium-PRPP and magnesium-PP_i are the true substrates for OPRTase, whereas orotate and OMP bind without being complexed to metal. EPR data gave no clear evidence of metal binding to enzyme, and the decrease in amplitude can be ascribed to a viscosity effect. From the Debye approximation (equation 13) we see a direct proportionality between τ_c and viscosity (η).

$$\tau_c = \frac{4\pi a^{*3}\eta}{3kT} \qquad (13)$$

Hence, an increase in viscosity will cause an increase in τ_c affecting the amplitude of the EPR signal (79). From the PRR data we see that the enzyme binds divalent metal cooperatively, and there may be two sites for metal on the enzyme, one an allosteric site, and another which binds the metal complexed to the substrate.

The observed decrease in e_b by the complexation of Mn^{2+} to the enzyme gives indication of a cooperative binding event. This same effect was reported with malate dehydrogenase (80), where binding of the paramagnetic probe initially gave a large e_b which decreased by a factor of ten as the two tight binding sites were filled. This allosteric metal site on OPRTase explains the lack of OMP-^{14}[C]-orotate exchange when the system was eluted through Chelex-100 to remove the metal. Two binding sites for metal have recently been detected for anthrinilate PRTase using PRR techniques (81). Extensive studies of the ternary complexes will have to be carried out to clarify the role of the metal-enzyme complexes in the presence of substrate for the proposed ping-pong mechanism of OPRTase.

The main objection to a ping-pong mechanism for phosphoribosyltransferase enzymes is the stereochemical argument that simple double-displacement mechanisms usually lead to retention of configuration in the products and phosphoribosyltransferases catalyze an inversion of configuration (75). In fact, stereochemical considerations, alone, have been utilized to outline an SN_2 mechanism for action for OPRTase (82). Because the ping-pong mechanism for OPRTase from yeast has been established in this work, a mechanism of action more complicated than double-displacement must be proposed. Two such mechanisms, described as Triple SN_2 and Carbonium Ion Formation, have been proposed (74) which are consistent with stereochemical inversion and an enzyme-phosphoribose intermediate. Kosower specifically suggested an enzyme-catalyzed SN_1 ionization of Mg^{2+}-PRPP with Mg^{2+}-PP_i as a leaving group resulting in a ribose-phosphate carbonium ion moiety left on the OPRTase. The orotate then attacks as a nucleophile forming OMP (83). Isotope

effect studies of Parsons (37) favor the carbonium ion intermediate as the mechanism by which OMP is formed in yeast. (He also detected a carbonium ion intermediate in hypoxanthine-guanine PRTase and ATP PRTase, as well.)

A mechanism of action which includes both a carbonium ion intermediate and the ping-pong kinetic mechanism is illustrated in Figure 21. The essential features of our proposed mechanism are as follows. The 3'-endo puckered ribofuranoside ring of PRPP is stabilized through interaction of a divalent metal ion with pyrophosphate and the C2' hydroxyl of the ring. The enzyme, with the allosteric metal already bound, is in the proper conformation to allow binding of the substrate metal complex. On the enzyme the furanose ring may assume a relatively unstable planer conformation, whereas the metal ion-pyrophosphate group is placed in a position for dissociation from the complex. Carbonium ion formation then may proceed within this planer ring, along with pyrophosphate departure, and amino acid residues which previously complexed with the metal may now be able to stabilize the carbonium ion. The glycosidic bond may then form from orotate with the stereospecificity dictated by the active site geometry, namely, the positioning of the base ring in the β -position relative to the ring carbonium ion.

An indirect consequence of this mechanism is that a covalent link between the furanose carbonium ion and the enzyme has not been postulated. However, sufficient nucleophilic groups may be present on PRPP to extend the lifetime of the intermediate at the active site long enough to allow the reaction to proceed. Such an intermediate may not have a sufficiently long half-life to allow for its isolation. This would explain our inability to conclusively detect the intermediate

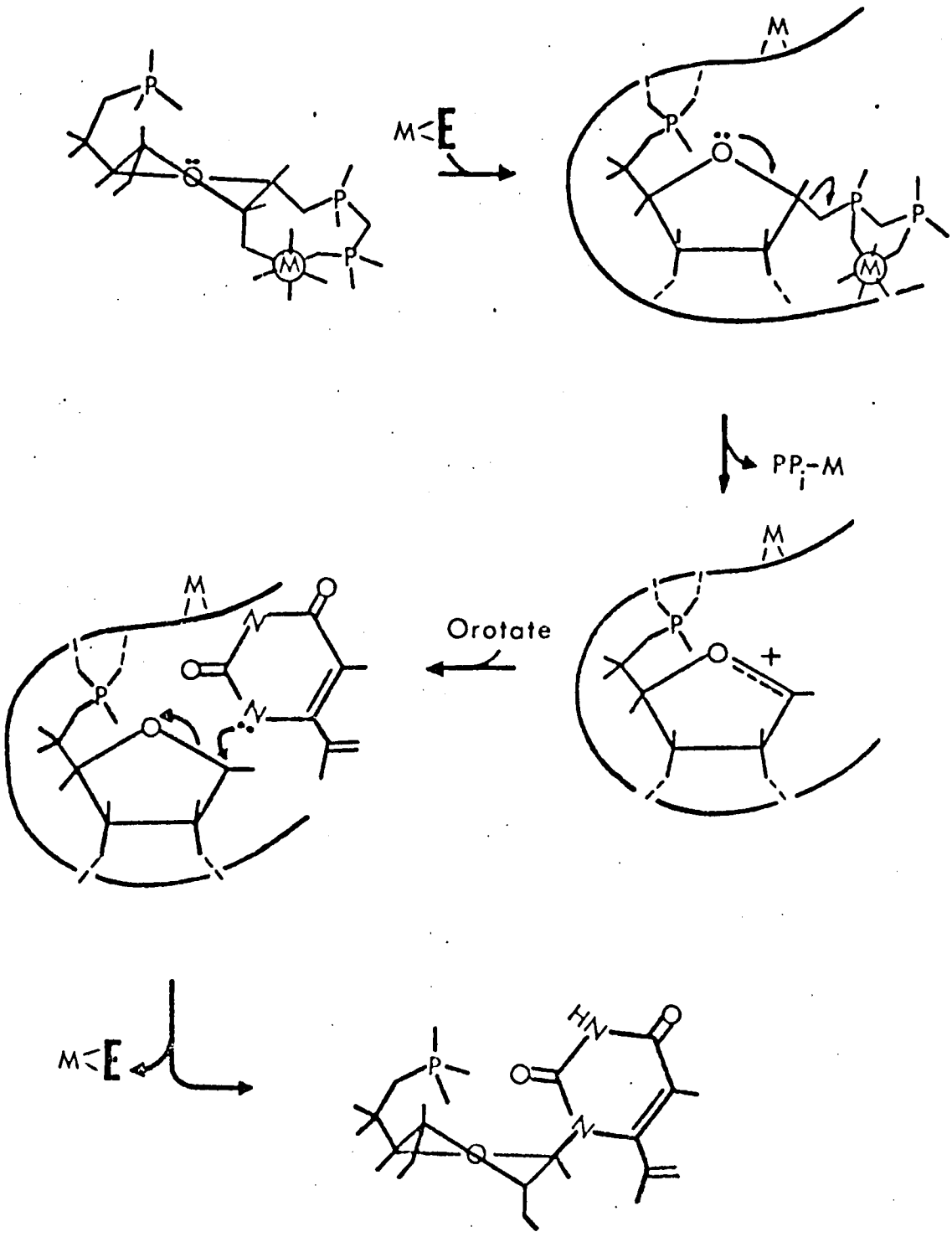

Figure 21. Proposed mechanism of OPRTase.

using molecular sieve chromatography.

Precedents for the use of ring carbonium ions in the enzymic hydrolysis of the C-1 position on glucose have been established for α and β amylase (84, 85) and for lysozyme (86). In addition, the acid catalyzed hydrolysis of glucose-1-phosphate appears to proceed by way of a cyclic carbonium ion (87) as does the reaction of methanol with 2,3,4,6 tetra-O-methyl α-D-glucopyranosyl chloride (88). Moreover, this latter reaction leads to an inversion of configuration (88), as does the reaction catalyzed by β-amylase (85).

The mechanism presented in Figure 21 is likely for orotate phosphoribosyltransferase from yeast. It is consistent with the kinetic, isotope exchange, EPR and PRR studies presented in this work. In conclusion, there now appears to be considerable evidence that living organisms may employ many different mechanisms for producing various nucleotides from PRPP, and in fact, a single organism may use these different mechanisms as a way of controlling the use of this important metabolite and allocating it among various biosynthetic pathways.

BIBLIOGRAPHY

1. Jones, M. E. (1971) Adv. in Enzyme Reg. 9, 19-49.
2. Lieberman, I., Kornberg, A., and Simms, E. S. (1955) J. Biol. Chem. 215, 403-415.
3. Kapoor, M. and Yaygood, E. R. (1965) Can. J. Biochem. 43, 143-164.
4. Umezu, K., Amaya, T., Yashismoto, A., and Tomita, K. (1971) J. Biochem. (Tokyo) 70, 249-262.
5. Appel, S. H. (1968) J. Biol. Chem. 243, 3924-3929.
6. Hatfield, D. and Wyngaarden, J. B. (1964) J. Biol. Chem. 239, 2580-2586.
7. Pinsky, L. and Kooth, R. S. K. (1967) Proc. Natl. Acad. Sci. U.S. 57, 925-932, 1267-1279.
8. Kasbekar, D. K., Nagabhushanam, A., and Greenberg, D. M. (1964) J. Biol. Chem. 239, 4245-4249.
9. Kavipurapu, P. R. and Jones, M. E. (1976) J. Biol. Chem. 251, 5589-5599.
10. Reyes, P. and Guganig, M. E. (1975) J. Biol. Chem. 250, 5097-5108.
11. Sweeney, M. J., Parton, J. W., and Hoffman, D. H. (1974) Adv. in Enzyme Reg. 12, 385-396.
12. Pausch, J., Keppler, D., and Decker, K. (1972) Biochim. Biophys. Acta. 258, 395-403.
13. Reyes, P. and Intress, C. (1978) Life Sci. 22, 577-582.
14. Foster, D. M., Lee, C. S., and O'Sullivan, W. J. (1973) Biochem. Med. 7, 61-67.
15. Tax, W. J. M., Veerkamp, J. H., and Trijbels, J. M. F. Comp. Biochem. Phys. B (1976) 54, 209-212.

16. Kornberg, A. (1962) in Horizons in Biochemistry (Kasha, M. and Pullman, B., eds.) pp. 251-264, Academic Press, New York.

17. Traut, T. W. and Jones, M. E. (1977) J. Biol. Chem. 252, 8374-8381.

18. Reyes, P. (1977) Anal. Biochem. 77, 363-369.

19. Brown, G. K. and O'Sullivan, W. J. (1977) Biochem. 16, 3235-3242.

20. Reyes, P., Intress, C., and Sandquist, R. B. (1978) Fed. Proc. 37, 1342.

21. Jones, M. E. (1972) Current Topics in Cellular Regulation (Horecker, B. L. and Stadtman, E. R., eds.) Vol. 6, pp. 227-265, Academic Press, New York.

22. Shoaf, W. T. and Jones, M. E. (1973) Biochemistry 12, 4039-4051.

23. Hoogenraad, N. J. and Lee, D. C. (1974) J. Biol. Chem. 249, 2763-2768.

24. Decker, K., Pausch, J., Willkoning, J., and Keppler, D. (1974) Fed. Eur. Biochem. Soc. Proc. 32, 223-228.

25. Isaac, J. H. and Halloway, B. W. (1968) J. Bact. 96, 1732-1741.

26. Jund, R. and LaCroute, F. (1972) J. Bact. 109, 196-202.

27. Caroline, D. F. (1969) J. Bact. 100, 1371-1377.

28. Williams, J. C. and O'Donovan, G. A. (1973) J. Bact. 115, 1071-1076.

29. Taylor, A. L., Beckwith, J. R., Pardee, A. B., Austrian, R. A., and Jacob, F. (1964) J. Mol. Biol. 8, 771.

30. Beckwith, J. R., Pardee, A. B., Austrian, R. A., and Jacob, F. (1962) J. Mol. Biol. 5, 618-634.

31. Worthy, T. E., Grobner, W. and Kelley, W. N. (1974) Proc. Natl. Acad. Sci. U.S. 71, 3031-3035.

32. Smith, L. H., Huguley, C. M., and Bain, J. A. (1972) in The Metabolic Basis for Inherited Disease, 3rd Ed. (Stanbury, J. B., Wyngaarden, J. B., and Fedrickson, D. S., eds.) p. 1003, McGraw-Hill, New York.

33. Krenitsky, T. A., Papaioannou, R., and Elion, G. B. (1969) J. Biol. Chem. 244, 1263-1270.

34. Gadd, R. E. A. and Henderson, J. F. (1970) Can. J. Biochem. 48, 302-307.

35. Fox, I. H. and Kelley, W. N. (1971) Ann. Int. Med. 74, 424-433.

36. Breadmore, T. D., Cashman, J. S., and Kelley, W. N. (1971) J. Clin. Invest. 51, 1823-1832.

37. Goitlein, R. K., Chelsky, D., and Parsons, S. M. (1978) J. Biol. Chem. 253, 2963-2971.

38. Segel, I. H. (1975) in Enzyme Kinetics, Wiley-Interscience, New York, pp. 606-625.

39. Krenitsky, T. A. and Papaaionnou, R. (1968) J. Biol. Chem. 244, 1271-1277.

40. Baumann, P. and Wright, B. E. (1968) Biochemistry 7, 3653-3661.

41. Gold, M. H. and Segel, I. H. (1974) J. Biol. Chem. 249, 2417-2423.

42. Bar-Tana, J. and Cleland, W. W. (1974) J. Biol. Chem. 249, 1271-1276.

43. Segel, I. H. Ibid., p. 653-654.

44. Segel, I. H. Ibid., p. 855-856.

45. Mildvan, A. S. and Cohn, M. (1965) J. Biol. Chem. 240, 238-246.

46. Ingram, D. J. E. (1970) in Biological and Biochemical Applications of Electron Spin Resonance, pp. 1-38, A. Hilger, Ltd., London, England.

47. Ochiai, E. (1977) in Bioinorganic Chemistry, pp. 41-46, Allyn and Bacon, Inc., Boston, Massachusetts.

48. Cohn, M. and Townsend, J. (1954) Nature 173, 1090-1091.

49. Mildvan, A. S. and Cohn, M. (1963) Biochemistry, 2, 910-919.

50. Mildvan, A. S. and Engle, J. L. (1972) in Methods in Enzymology, Vol. 26, pp. 654-682, Academic Press, New York.

51. Bloombergen, N., Purcell, E. M., and Pound, R. V. (1948) Phys. Rev. 73, 679-712.

52. Ochiai, E., Ibid., pp. 388-392.

53. Sloan, D. L. and Mildvan, A. S. (1974) Biochemistry 13, 1711-1718.

54. Mildvan, A. S. and Weiner, H. (1969) Biochemistry, 8, 552-562.

55. Grisham, C. M. and Mildvan, A. S. (1974) J. Biol. Chem. 249, 3187-3197.

56. Reyes, P. and Sandquist, R. B. (1976) Fed. Proc. 35, 1752.

57. Dahl, J. L., Way, J. L., and Parks, R. G. (1959) J. Biol. Chem. 234, 2998-3002.

58. Lowry, O. H., Rosebrough, N. J., Farr, L., and Randall, R. J. (1951) J. Biol. Chem. 193, 265-275.

59. Davis, B. J. (1964) Ann. N. Y. Acad. Sci. 121, 404-427.

60. Weber, K. and Osborn, M. (1969) J. Biol. Chem. 244, 4406-4412.

61. Shapiro, A. L., Vinuela, E., and Maizel, J. V. (1967) Biochem. Biophys. Res. Comm. 28, 815-820.

62. Kornberg, A. (1950) J. Biol. Chem. 182, 779-793.

63. Brown, A. N. (1946) Arch. Biochem. 11, 269-278.

64. Reyes, P. (1972) Anal. Biochem. 50, 35-39.

65. Reyes, P. and Guganig, M. (1972) Anal. Biochem. 46, 276-286.

66. Horecker, B. L. (1957) in Methods in Enzymology, Vol. 3, p. 188, Academic Press, New York.

67. Hershko, A., Razin, A., and Mayer, J. (1969) Biochim. Biophys. Acta. 184, 64-76.

68. Flaks, J. G. (1963) in Methods in Enzymology, Vol. 6, pp. 473-479, Academic Press, New York.

69. Cleland, W. W. (1963) Biochim. Biophys. Acta. 67, 104-137.

70. Bell, R. M. and Koshland, D. S. (1970) Biochem. Biophys. Res. Comm. 38, 539-545.

71. Tebar, A. R., Ballesteros, A., and Soria, J. (1977) Experimentia, 33, 1292-1293.

72. Packman, P. M. and Jakoby, W. B. (1967) J. Biol. Chem. 242, 2075-2079.

73. Hori, M. and Henderson, J. F. (1966) J. Biol. Chem. 241, 3404-3408.

74. Chelsky, D. and Parsons, S. M. (1975) J. Biol. Chem. 250, 5669-5673.

75. Brashear, W. T. and Parsons, S. M. (1975) J. Biol. Chem. 250, 6885-6890.

76. Morton, D. P. and Parsons, S. M. (1976) Arch. Biochem. Biophys. 175, 677-686.

77. Kleeman, J. E. and Parsons, S. M. (1976) Arch. Biochem. Biophys. 175, 687-693.

78. Henderson, J. F., Brox, L. W., Kelley, N. N., Rosenbloom, F. M., and Seegmiller, E. (1968) J. Biol. Chem. 243, 2514-2522.

79. Hertz, H. G. (1967) in Progress in NMR Spectroscopy, Vol. 3, p. 171 (Emsley, J. W., Feeney, J., and Sutcliffe, L. H., eds.), Pergamon Press, New York.

80. Mildvan, A. S., Waber, L., Villafranca, J. J., and Weiner, H. (1972) in Structure and Function of Oxidation-Reduction Enzymes, pp. 745-754 (Akeson, A. and Ehrenberg, A., eds.), Pergamon Press, New York.

81. Robison, P. D., Nowak, T., and Levy, H. R. (1978) Fed. Proc. 37, 1620.

82. Kaneti, J., Golovinsky, E., Yulchnovsky, I., and Ganchev, D. (1970) J. Theoret. Biol. 26, 19-27.

83. Kosower, E. M. (1962) in Molecular Biochemistry, pp. 39, 261-262, McGraw-Hill, New York.

84. Mayer, F. C. and Larner, J. (1958) Biochim. Biophys. Acta. 29, 465.

85. Thoma, J. A. (1968) J. Theoret. Biol. 19, 297-310.

86. Imoto, T., Johnson, L. N., North, A. C. T., Phillips, D. C., and Rupley, J. A. (1972) in The Enzymes, 3rd Ed. (Boyer, P. D., ed.), Vol. 7, Chapter 21, Academic Press, New York.

87. Banks, B. E. C., Meinwald, Y., Rhind-Tutt, A. J., Sheft, I., and Vernon, C. A. (1961) J. Chem. Soc., 3240-3246.

88. Rhind-Tutt, A. J. and Vernon, C. A. (1960) J. Chem. Soc., 4637-4645.

CURRICULUM VITAE

NAME: Jacob Victor

ADDRESS: 83-30 118th Street, Kew Gardens, New York 11415

TELEPHONE NO.: (212) 847-1436

BIRTHDATE: June 12, 1951

CITIZENSHIP: U.S.A.

EDUCATION:

Undergraduate: B.S., Chemistry, City College of New York, 1973

Graduate: Ph.D., Biochemistry, City University of N.Y., 1978

TEACHING EXPERIENCE: Teaching Fellowship--City College of N.Y., 1973-77

ACADEMIC HONORS:

Undergraduate: Phi Beta Kappa, 1973
Alpha Sigma Lambda, 1973
New York State Regents Scholarship, 1969-1973

PROFESSIONAL SOCIETIES: Sigma Xi, 1978
American Association for the Advancement of Science, 1978

PUBLICATIONS: Federation Proceedings (1978) 37, abstract #2938, "Kinetic Mechanism of Orotate Phosphoribosyltransferase from Yeast," J. Victor, L. Greenberg, and D. L. Sloan.